Theses and Dissertations

Spring 2011

Road variability and its effect on vehicle dynamics simulation

Amit Udas
University of Iowa

Recommended Citation

Udas, Amit. "Road variability and its effect on vehicle dynamics simulation." MS (Master of Science) thesis, University of Iowa, 2011.
http://ir.uiowa.edu/etd/1097.

ROAD VARIABILITY AND ITS EFFECT ON VEHICLE DYNAMICS SIMULATION

by

Amit Udas

A thesis submitted in partial fulfillment
of the requirements for the Master of
Science degree in Mechanical Engineering
in the Graduate College of
The University of Iowa

May 2011

Thesis Supervisor: Professor Emeritus Lea-Der Chen

Graduate College
The University of Iowa
Iowa City, Iowa

CERTIFICATE OF APPROVAL

_____

MASTER'S THESIS

_____

This is to certify that the Master's thesis of

Amit Udas

has been approved by the Examining Committee
for the thesis requirement for the Master of Science
degree in Mechanical Engineering at the May 2011 graduation.

Thesis Committee: _____
                              Lea-Der Chen, Thesis Supervisor

                              _____
                              Shaoping Xiao

                              _____
                              Jia Lu

                              _____
                              Joe Kleiss

ACKNOWLEDGMENTS

ABSTRACT

In the modern age, computer aided engineering software is used in nearly every engineering design application. In this thesis, a multibody dynamics vehicle model in LMS Virtual.Lab simulation platform was updated. The updates included measured hardpoint data of the vehicle studied, addition of two differential gear models to the vehicle drivetrain, and implementation of a multibody dynamics model of a trailer that is attached to the vehicle. To extend the length of the experimentally acquired road profile, a distribution function based methodology was developed to create road profile from the limited road data. The road parameter generated from the distribution function was used to recreate a road profile statistically representative of acquired road profile data. The updated vehicle dynamics model was validated by comparing the simulation results to the vehicle dynamics test results conducted at the Nevada Automotive Test Center. To validate the methodology for creating the road profile, vehicle dynamics simulation results with the distribution function generated road profile were compared to the results from the acquired road profile. The effects of road variability on the vehicle dynamics simulation were also examined. By using a Gamma distribution to define the road roughness, a sensitivity analysis was conducted to study how the variation in road roughness affects the vertical, longitudinal and lateral accelerations at the driver's location. The results show that the RMS values of the acceleration increase linearly with increasing mean roughness for variance up to $\pm30\%$ and a quadratic response for variance up to $\pm100\%$.

TABLE OF CONTENTS

LIST OF TABLES

Table

LIST OF FIGURES

LIST OF NOMENCLATURE

B	Beta Function
CRMS	Control RMS
D	Kolmogorov-Smirnov statistic
F	Theoretical cumulative distribution function
h	Time step size
k	Continuous shape parameter
$\boldsymbol{M}$	Maxx matrix of bodies
m	Order of polynomial fit
MAX	Maximum
MIN	Minimum
N, n	Total number of data points
ORMS	Observed RMS
PCMR	Percent change in mean roughness
PCRMS	Percent change in RMS
RMS	Root mean square
$\boldsymbol{Q}$	Vector of applied forces
$\boldsymbol{q}_i$	Cartesian coordinates for each body in the model. NB refers to total number of bodies present in the model
$\dot{\boldsymbol{q}}$, $\ddot{\boldsymbol{q}}$	First and second time directive, respectively
R^2	Correlation of determination
S_{yx}	Standard error of the fit
t	Time
$Var(x)$	Variance
X, x	State variables

y_i	Data points
z_i	Observed value
z_c	Predicted value from the polynomial fit
$\bar{x}$	Mean
3P	Three Parameter
4P	Four Parameter

Greek Symbols

$\alpha, \alpha_1, \alpha_2$	Continuous shape parameter
β	Continuous location scale parameter
Γ	Gamma Function
γ	Second derivative of the constraint equations
δ	Continuous parameter
η	Continuous parameter
λ	Lagrange multipliers
μ	Continuous parameter
ν	Degrees of freedom of the fit
ξ	Continuous parameter
π	Mathematical constant pi
σ	Continuous shape parameter
ς	Continuous location parameter
τ	Continuous location parameter
$\boldsymbol{\Phi}_q$	Algebraic constraints used to restrict motion and subscript denotes a partial differentiation

CHAPTER 1

INTRODUCTION

1.1 Background

Simulation power of computer-aided engineering (CAE) software increases every

day. Tasks used to take days to complete can be completed in hours with the help of

more powerful processors and efficient software. CAE software is used in all aspects of

designing a new product. Rather than constructing and testing multiple physical

prototypes, most products are now created and tested virtually. These products are

optimized using the CAE software until a satisfactory model is created and at which point

a prototype is created and physically tested. Commercial software like LMS Virtual.Lab

(LMS, 2010) is capable of performing a wide range of analysis including multibody

dynamics, finite element analysis, optimization and sensitivity analysis etc. Virtual

models can be used to supplement or replace physical testing during the product

development. For example, procedures given in MIL-STD-810G (2008), which consists

of standards for testing, must be followed for testing of military vehicles. Physical

testing is an effective means to verify that the products meet the required specifications.

However, it is often time consuming and expensive. For vehicle testing, the results are

subjected to uncertainties due to variances in environmental (e.g., road conditions) and

operating (e.g., driver input) conditions. Quantifying these uncertainties require multiple

tests that result in higher costs and longer time for product verification. Simulation-based

testing and verification can reduce the time and cost in the test process. For simulation-

based vehicle testing, error sources include variances in vehicle geometric parameters,

vehicle suspension parameters, tire properties, powertrain, material properties, driver

model, and road profiles. The primary concern of this thesis is the road profiles. Experimentally determined road profiles are often of a limited driving range. However to complete a mission profile in a simulation environment beyond the range of experimentally acquired road profiles, extension of the road profile data is needed. This thesis focuses on the development of a distribution function based methodology to create road profile from a limited set of road data for simulation environment. Using the created road profiles, assessments of road profile sensitivity on vehicle models are studied.

1.2 Objective

MIL-STD-810 G (2008) is a set of military standards that specifies the vehicle testing conditions including specifications of driving on test tracks. To develop enabling technologies for testing in a simulation environment, the specific objective of this thesis is to develop a methodology that simulates the test track characteristics for testing in a simulation environment. A distribution function based methodology was adopted. Using this methodology, road profiles were extended beyond the limited data acquired from the test tracks. A multibody dynamics vehicle model in LMS Virtual.Lab simulation platform was developed. The model was based on an earlier model reported by Zeman (2009). The updates included measured hardpoint data of the vehicle studied, addition of two differential gear models to the vehicle drivetrain, and implementation of a multibody dynamics model of a trailer that is attached to the vehicle. A parametric study was also conducted to study the effects of road roughness on vehicle dynamics simulation as quantified by RMS values of the vertical, longitudinal and lateral accelerations at the driver's location.

1.3 Literature Review

Ever since the invention of modern vehicles, quantification of road roughness has been of great interest. Road profile is a two-dimensional slice of a road surfaces, taken along an imaginary line. Figure 1-1 shows longitudinal and lateral profiles on a road surface. Profiles taken along a lateral line show the elevation changes across the road, while longitudinal profiles show the roughness of the road.
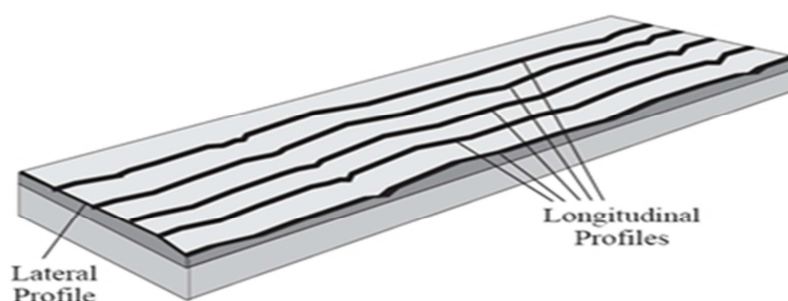
Figure 1-1: Road Profile (Michael, 1998)

Profilers are devices used to measure road profiles. There are many types of profilers and they differ by the resolution, the interval of measurements recorded, and the speed at which the profiler is able to take measurements. A profiler works by combining a reference elevation, a height relative to that reference, and longitudinal distance (Michael, 1998). A device, called a rod and level, forms a basic profiler shown in Figure 1-2. The level provides the height reference, and the reading from the rod is the elevation change relative to the reference. The longitudinal measurements between the rod and the level are taken with a tape measure or a laser. The rod and level is a static method because the instruments are not moving when taking measurements.
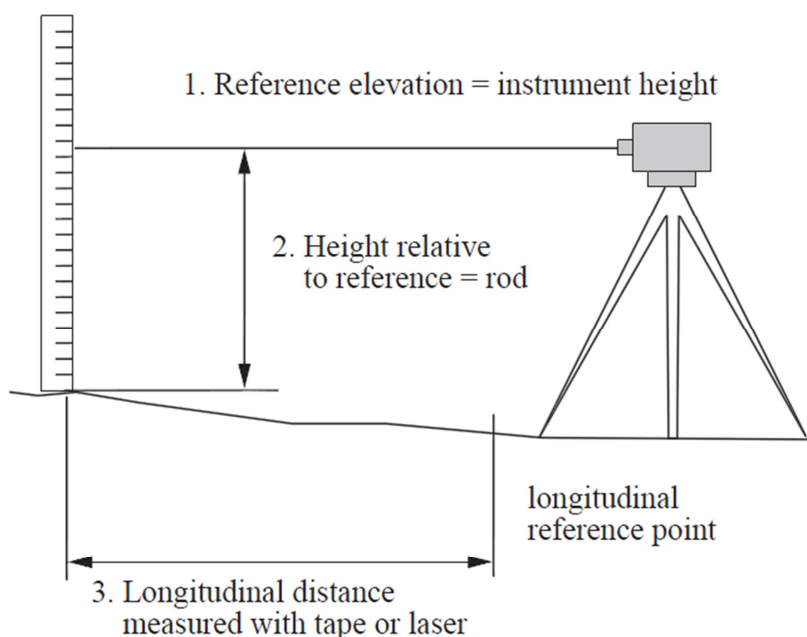
Figure 1-2: Rod and Level (Michael, 1998)

In 1960's, General Motors Research Laboratories developed the inertial profiler that made high-speed profiling possible (Michael, 1998). An accelerometer mounted on a moving vehicle measures the vertical acceleration. A computer processes the data and with reference to an inertial reference height, the elevation change of the accelerometer in the host vehicle is defined. Combining the accelerometer data, a laser transducer that measures the roughness of the road and the vehicle speed from the speedometer, high-speed profiling is possible. This is significant because the development of the inertial profiler made monitoring large road networks possible.

Even though models have been created to describe road profiles since the early 1970s, only recent technology advancements have allowed to gather comprehensive data to analyze road profile thoroughly. New laser profilers have made it possible to get high

speed profiling with high resolution and small sampling intervals. The laser readings coupled with the vertical acceleration data enables estimates of roughness resolution of 0.2 mm and sampling interval of 50 mm (Rouillard, 2001). It was shown by Perm (1988) that the laser profiler is valid for wavelengths ranging from 0.2 to 33 m. This range corresponds to a wavelength bandwidth at which vehicle vibrations are significant for typical vehicle speeds.

Dodds and Robson (1973) were among the first to conduct extended study of road surfaces. They proposed that typical road surfaces may be considered a homogeneous and isotropic random process with a Gaussian distribution. A single-track power spectral density (PSD) estimate can be used to generate a complete description of a typical road. It was also shown that the shape of the road data PSD estimates is independent of the road type and is a function of the RMS (root mean square) of road roughness.

Heath (1989) proposed a modification to the isotropic roughness assumption of Dodds and Robson (1973). Heath concluded that the entire roads were not completely homogeneous and only certain sections of roads were found to be homogeneous. Furthermore, Heath (1988) and Rouillard et al. (1996) showed that distribution of typical road surface roughness deviates from the Gaussian distribution and needs further investigation to provide a model for accurate road roughness description.

Bruscella et al. (1999) recommended that road surface classification cannot be based on spectral characteristics alone for vehicle simulation. Classification of road profiles is better achieved by using spatial acceleration because transient events are more easily identified in thee spatial acceleration domain. A method of separating the non-

Gaussian and transient characteristics from the Gaussian characteristics of road profile is required.

Rouillard et al. (2001) proposed a concept of treating road surface irregularities as two fundamental components: the underlying stationary, i.e., does not change when shifted in time or space, road surface irregularities and the transient events. It was shown that the underlying roughness profile can be described by an offset Rayleigh distribution and was a function of the RMS of the roughness. The transient events, which are the second fundamental component, were generated by a Gaussian distribution. The mean and standard deviation of this Gaussian distribution were a function of RMS level of the underlying roughness profile (Rouillard, 2001). The two components are combined to characterize a comprehensive representation of road surface irregularities.

Bogsjo (2006) proposed a similar concept of treating road surface by separating the irregularities into stationary and non-stationary components. The general roughness is modeled by a stationary Gaussian process. To model the occurrence of unusually rough parts, random irregularities are superimposed to the stationary process at random locations (Bogsjo, 2006). Two types of irregularities are superimposed: long-wave and short-wave. The long-wave represents the elevation changes due to terrain variations and the short-wave represents the high roughness parts of the road.

Kang et al. (2009) developed a vehicle simulation environment for evaluating durability of the suspension elements. Tire model with its complex nonlinear characteristics has significant impact on the credibility of durability analysis. The proposed method generates an equivalent road profile to compensate for the inadequate tire model. First the method identifies the frequency response function from the road

height to spindle force and then back-calculates a road profile. The solution is updated iteratively until it yields the spindle forces close to the measured value. Using this method for back-calculating a road profile, a durability analysis was performed for a suspension component. It was found that the estimated fatigue life using the simulation results agreed well with the estimation based upon the force measurement with only 9% difference between the results (Kang, 2009).

Improvements have been made in the methods for describing the road profiles but little is known about how uncertainties of the road profile affect the results from a vehicle simulation model. Using similar ideas from Rouillard (2001) and Bogsjo (2006), a methodology for creating road profiles by combining different aspects of the road roughness is developed. Using this methodology this thesis studies the effects of varying road profiles on vehicle dynamics simulation.

CHAPTER 2

CAE SOFTWARE AND VEHICLE MODEL

2.1 CAE Software

LMS Virtual.Lab is a powerful engineering software. It offers a wide variety of analysis options for design assessments. Virtual.Lab integrates many types of CAE software and is suited for multibody models that require finite element, acoustics, noise and vibration, and durability and optimization analysis. In this thesis LMS Virtual.Lab Rev 9-SL1 is used to update an earlier HMMWV (High Mobility Multipurpose Wheeled Vehicle) model (Zeman, 2009). HMMWV is a military vehicle. A picture of a generic HMMWV is shown in Figure 2-1. The multibody dynamic capabilities of Virtual.Lab Motion - Mechanism Design (LMS, 2010) were used to update and add additional components to the earlier model (Zeman, 2009).

Figure 2-1: HMMWV (source: www.defense-update.com)

2.2 Virtual.Lab Solver

Virtual.Lab uses the Euler-Lagrange formulation to construct the equations of motion. Each body in the model is located by Cartesian coordinates ($\boldsymbol{q}_i$) and assembled as shown in Equation (2-1):

$$\boldsymbol{q} = [\boldsymbol{q}_1^T, \boldsymbol{q}_2^T, \dots \boldsymbol{q}_{NB}^T]^T \tag{2-1}$$

where NB denotes the total number of bodies in the model.

Algebraic constraints $\boldsymbol{\Phi}(\boldsymbol{q})$ are used to restrict the motion and eliminate degrees of freedom from the system specified by the joint definitions. Lagrange multipliers, λ, are used to append the algebraic constraints to the equations of motion, which results in a set of differential-algebraic equations (Prescott and Laughlin, 2006). The constrained equations of motion are given by Equations (2-2) and (2-3) where $\boldsymbol{M}$ is the mass matrix of the bodies, $\boldsymbol{\Phi}(\boldsymbol{q})$ are the algebraic constraints, $\boldsymbol{Q}$ is the vector of applied forces, γ is the second derivative of the constraint equations, and X represents the state variables.

$$\begin{bmatrix} \boldsymbol{M} & \boldsymbol{\Phi}_q^T \\ \boldsymbol{\Phi}_q & 0 \end{bmatrix} \begin{bmatrix} \ddot{q} \\ \lambda \end{bmatrix} = \begin{bmatrix} \boldsymbol{Q} \\ \gamma \end{bmatrix} \tag{2-2}$$

$$\dot{X} = \dot{f}(\boldsymbol{q}, \dot{\boldsymbol{q}}, \ddot{\boldsymbol{q}}, \lambda, X) \tag{2-3}$$

The constraint equations are given in Equations (2-4) to (2-6) (Haug, 1989).

$$\boldsymbol{\Phi}(\boldsymbol{q}) = 0 \tag{2-4}$$

$$\boldsymbol{\Phi}_q \dot{\boldsymbol{q}} = 0 \tag{2-5}$$

$$\boldsymbol{\Phi}_q \ddot{\boldsymbol{q}} + (\boldsymbol{\Phi}_q \dot{\boldsymbol{q}})_q \, \dot{\boldsymbol{q}} = 0 \tag{2-6}$$

Note that bold font indicates the given quantity is a vector, the subscript denotes a partial differentiation and the over dot signifies a differentiation with respect to time.

User input includes the analysis type (e.g., static, kinematic, dynamic), simulation time, the print interval for the results to be recorded, the solution tolerance, the maximum integration steps, integration tolerance and acceleration tolerance for the solver to satisfy when solving a model. Several numerical solvers are available to solve the equations of motion. Backward Difference Formula (BDF) solver is a second-order difference scheme and was chosen for this thesis. The BDF consists of a predictor and a corrector stage. The corrector goes through an iterative process until the residual is less than the tolerance specified by the user. This process is repeated for every time step during the simulation. Once the corrector has converged, the backward difference formula shown in Equation (2-7) is used to get the value for the next time step where x represents the state variables and h is the time step size.

$$F(t_i x_i \dot{x}_i) = F\left(t_i, x_i, \frac{x_i - x_{i-1}}{h_i}\right) = 0 \qquad (2\text{-}7)$$

When solving an analysis case in Virtual.Lab, the program writes an input file that is read by the solver. This file contains information regarding the properties of all the bodies in the model such as location information, mass properties, inertia data, joint definitions and other data necessary to solve the model. After a model solves correctly, the results are saved in a binary MotionResults file. This file is later read by Virtual.Lab for post-processing. When an error occurs while solving an analysis case, Virtual.Lab creates an error log under LMSMotionInfo.

2.3 Review of HMMWV Models

On March 1983, AM General was awarded the initial production contract for the HMMWV. On January 2nd, 1989 AM General released the first HMMWV. HMMWV is a light weight, highly mobile, 4 wheel drive, diesel powered tactical vehicle. It was

designed to be maintainable, reliable and survivable for military use. The vehicle could be constructed in multiple configurations on a common chassis to perform a wide variety of missions. Over 250,000 have been produced for the US and 50 other nations (AM General Website, 2010).

For a vehicle like the HMMWV, METHOD 541.6 in the MIL-STD-810G (MIL-STD-810G) describes the procedures for acquiring the vibration data for the life cycle evaluation. Depending upon the scenarios to be simulated, the vehicles will be required to travel thousands of miles on interstate highways and off-road courses. Vehicles are sometimes tested on rougher terrains and driven at faster speeds to simulate the wear of vehicles that have been driven for longer distances. The costs associated with these accelerated test runs are enormous. These tests are needed when significant changes to the vehicle are implemented, making it an expensive and time demanding procedure. The advantages of a virtual proving ground can readily be seen as the testing is conducted in a simulation environment. Key to the validity of testing in a virtual proving ground is the validated simulation capabilities.

Many efforts have been made over the recent years to accurately model a vehicle in simulation environment. There are five main components to building an accurate vehicle model: the vehicle geometric parameters, the material parameters, the tire element, the suspension element and the road element. Each component has been studied in detail but simplifications are still needed for full vehicle simulation with currently available computing resources.

Most vehicle handling simulations are conducted on flat surfaces. The tire models used in those types of simulations only have contact with the ground at a single

point. For simulation on flat surfaces, this approach works well but the actual contact between a tire and road occurs over a distributed area. Mousseau et al. (1999) made efforts to improve the performance of the tire element by modeling tires using the nonlinear finite element (FE) method. The results from the integration of the tire modeled using FE and a rigid body vehicle model showed great correlation when compared with experimental results of similar tests. The test runs included the vehicle running over a 25 mm high step and a chuckhole which was 0.76 m long and 0.1 m deep. This type of high fidelity model takes hours of CPU time for a few seconds of wall-clock time simulation. For simulation of vehicle was driving over the chuckhole, 9 seconds of simulation took 13.5 CPU hours on a two processor SGI workstation with shared memory (Mousseau et al., 1999).

High fidelity analysis can be extended into the suspension of the model where the majority of the vehicle suspension is built using FE methods. Hussien et al. (2010) developed a detailed FE model for the rear axle system of a sport utility vehicle. The multibody system consisted of nine bodies and used a non-conventional finite element formulation, which was used to develop the equations of motion of the rotating input and output shafts to account for the effects of the angular velocities. The model includes the effects of the bearing stiffness, the springs in the suspension, and the stiffness of the tires. The results showed that the velocities of the rotating shafts become significant at higher vehicle velocities, e.g., over 1000 rad/s. The results also show that increasing the mass density of both the carrier and the differential gears leads to the decrease in of the system natural frequencies. The carrier inertia had a significant effect on the first six modes,

while the inertia of the differential gears affected the first, second, and fourth modes

(Hussien et al., 2010).

The HMMWV model used in this study was built upon Zeman's thesis (Zeman,

2009). Zeman modeled the HMMWV with 68 bodies. The model included front and rear

suspensions, steering system, a torque based transmission, and a simplified tire model.

The stiffness and damping coefficients of the suspension were experimentally determined

by conducting measurements of actual springs and dampers taken from a HMMWV. The

simplified tire model was based on the Complex Tire model of Virtual.Lab. The steering

and torque transmission models were also generic models given in Virtual.Lab. The

vehicle geometric parameters, i.e., the hard points that connect the suspension

components and chassis parameters were taken from a 1988 report (Aardema, 1998).

The hard points and the transmission are updated in this thesis.

2.4 HMMWV Model built in Virtual.Lab

To model the front suspension, upper and lower control arms, an upper and lower

damper, steering knuckle, spindle, hub and wheel were required on each side. Figure 2-2

shows an upper-level topology of the front suspension system. The numbering of the

bodies represents the body numbers in Table 2-1. Note that not all bodies are included in

this topology for simplicity. The suspension system in Virtual.Lab can be created using a

suspension subsystem program which creates suspension components with different

levels of complexity. Depending on the complexity of the suspension system,

Virtual.Lab creates the necessary bodies to construct the model. The subsystem requires

hardpoints, which are the coordinates of the suspension components and the connecting

points for the joints. These hardpoints are created according to the coordinate system

used in the vehicle model. Other information required to construct a suspension system include stiffness for springs and dampers, tire properties and other parameters depending on the complexity of the suspension. Several parameters like the free length of the spring and damper are automatically tabulated by the subsystem based on the hardpoints.

Table 2-1: Vehicle Topology Body Numbering

Body Number	Body Name
1	Chassis
2	Front Left Lower Control Arm
3	Front Left Upper Control Arm
4	Front Left Steering Knuckle
5	Front Left Spindle
6	Front Left Hub
7	Front Left Wheel
8	Front Left Tierod
9	Front Right Tierod
10	Centerlink
11	Pitman Arm
12	Idler Arm
13	Steering Gearbox
14	Pinion Gear
15	Steering Shaft
16	Steering Wheel
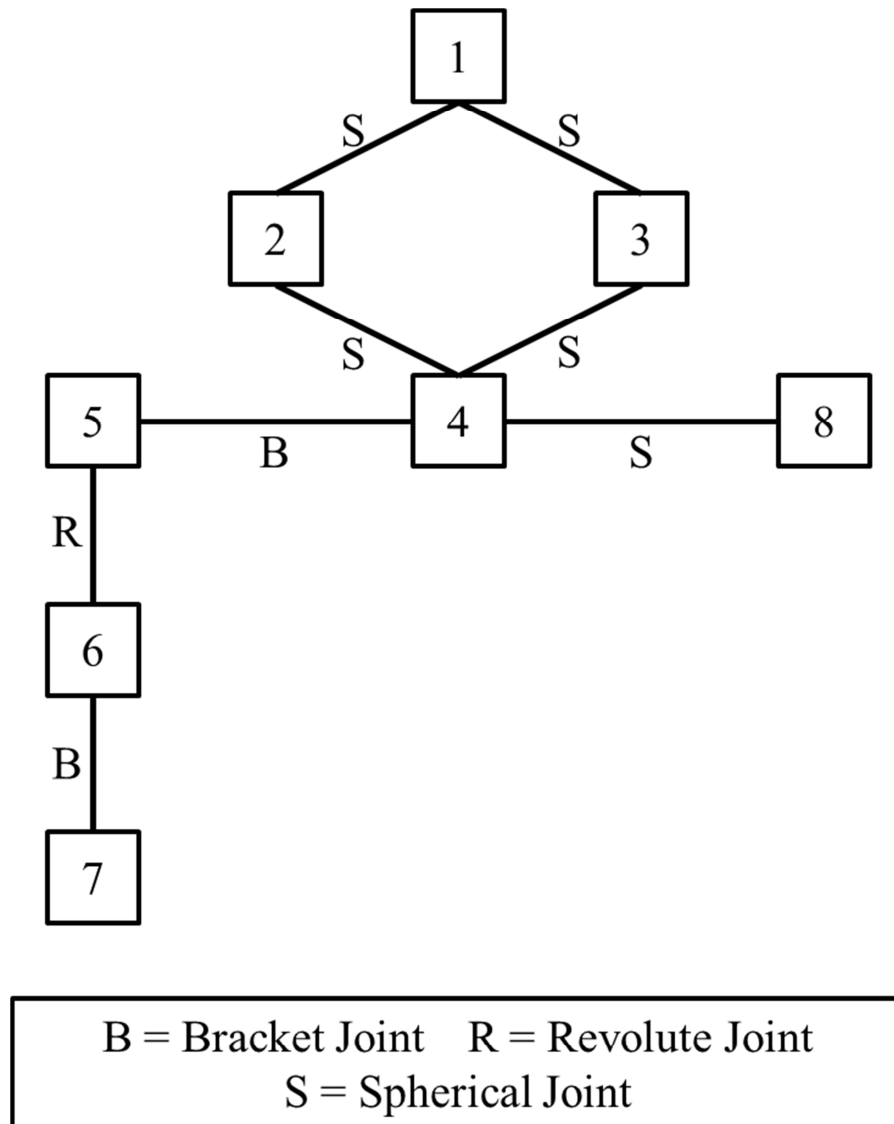
Figure 2-2: Vehicle Suspension Topology

The steering subsystem was used to connect the steering mechanism to the front suspension. A tierod between the knuckle and the centerlink of the steering system was used to constrain the steering angle of the wheels. The properties of the steering systems used by Zeman (2009) were used. The steering subsystem topology can be seen in Figure 2-3. Again, the numbering of the bodies represents the body numbering in Table 2-1.
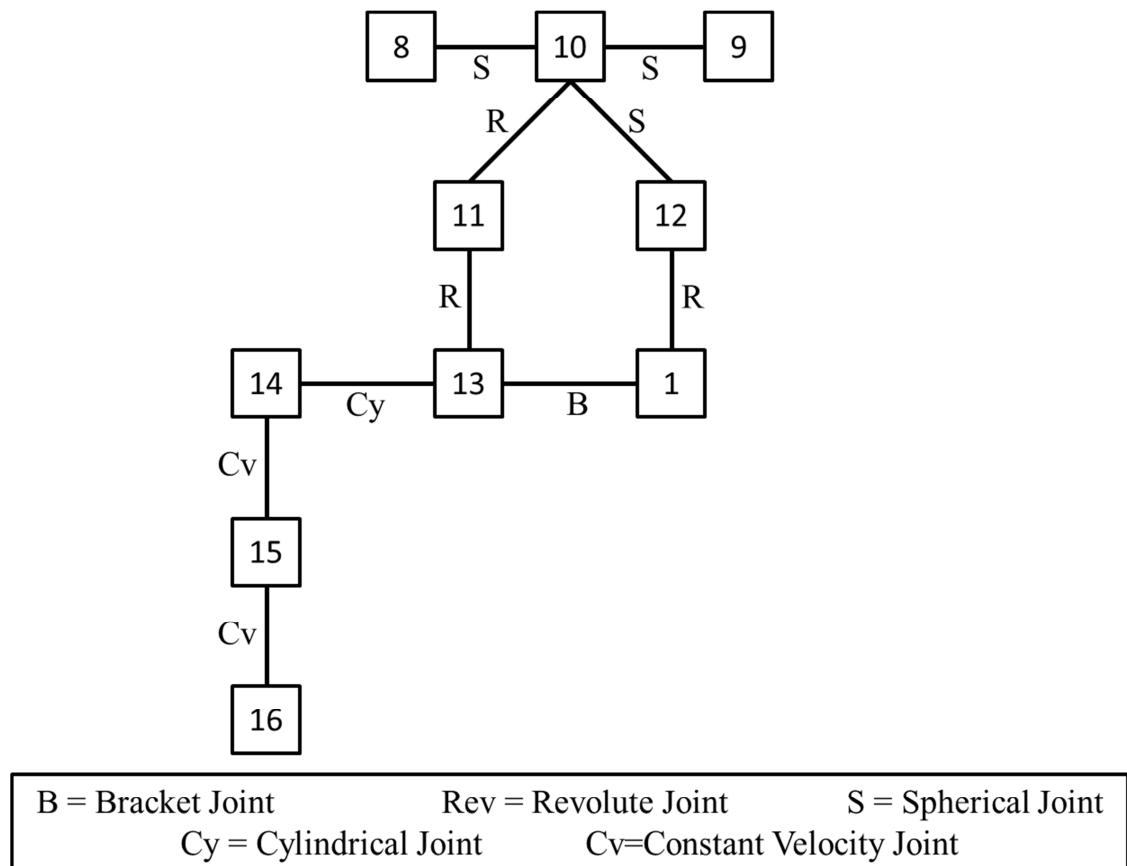
Figure 2-3: Vehicle Steering Topology

The rear suspension was created in a similar fashion with the exception of the connection to the steering system. In place of tie rods, radius rods were used to connect the knuckles to the chassis, which restrict steer motion of the rear wheels. All of the suspension components was modeled for only half of the vehicle and mirrored to the other side.

To model the HMMWV's fulltime all-wheel drive transmission, an all-wheel drivetrain was developed. Two differential gears were added to the drivetrain that drive the front and rear wheels. Both the differentials are driven by the same input and the power was distributed to all four wheels governed by the differential gears. Gear ratios for the differentials were taken from an actual differential from a HMMWV. The real differential has a pinion which is connected to the carrier, and has six spider gears that connect to the two side gears which are part of the axle going to the wheels. The differential model used is a simplified model that only utilizes two spider gears instead of six. Since the differential is built through kinematic constraints, the number of spider gears will not have an effect on how the differential performs. Finally the output axels from the differentials are connected to the wheels using a constant velocity joint so that the output from the differential is transferred straight to the wheels. To achieve the four wheel drive requirement, both front and rear pinions were driven from the same input using a gear joint. Figure 2-4 below shows the differential topology. The body numbering of the bodies represents the body numbering in Table 2-2. In order to connect the bodies using gear joints, revolute joints are first required to restrict the motion. Two revolute joints are required before a gear joint can be used. Four gear joints were used to create each of the differentials. A gear joint were created between the carrier and the

pinion, the spider gear 1 and the spider gear 2, spider gear 1 and left differential axel, and

the spider gear 2 and right differential axel.

Table 2-2: Differential Topology Body Numbering

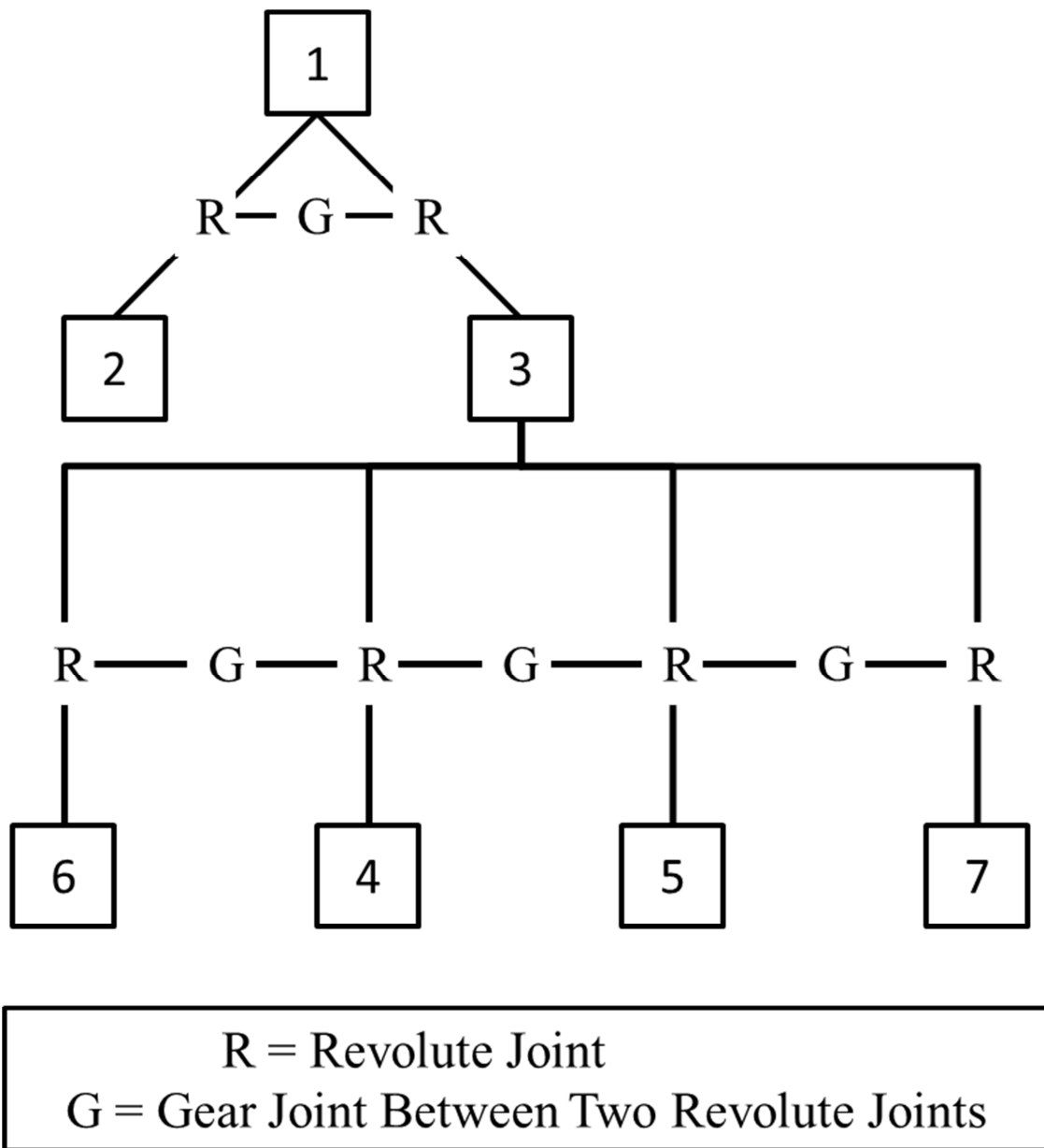| Body Number	Body Name
1	Chassis
2	Pinion
3	Carrier
4	Spider Gear 1
5	Spider Gear 2
6	Left Differential Axle
7	Right Differential Axle

Figure 2-4: Vehicle Differential Topology

2.5 Vehicle geometric parameter determination

The hardpoints used by Zeman (2009) were updated using data measured by a FaroArm (FaroArm Fusion, 2011). The FaroArm is a precision measurement device that is capable of measuring points in three dimensional space. The instrument is capable of measuring and comparing planes, edges, points and measuring simple geometries like a circle. The coordinates of the hardpoints are recorded relative to the device and is accurate to $\pm$ 0.0020 in (FaroArm Fusion, 2011). All of the hard points were taken with respect to the coordinate system created on the front drive axle in the center of the vehicle. The coordinate system is set up to follow the ISO vehicle coordinate system, in which the right-hand rule is used. Namely, the positive X-axis is pointing in front of the vehicle, positive Y-axis is pointing toward the right of the vehicle and Z-axis is pointing vertically upward. The origin of the axis system was set in this particular way to match how the hard points were gathered and entered in to create the HMMWV model.

In order to take the measurements of all the suspension components, the wheels in the front and the rear of the vehicle had to be removed. The ride height was first recorded before taking the wheels off so the vehicle could be elevated back to the proper ride height afterwards. Doing so enabled all of the components would be at ride height and also allowed easy access to all the suspension components with the FaroArm. The hardpoints for the trailer was also recorded using a similar procedure. The HMMWV model was updated with hardpoint data acquired

2.6 Trailer Model built in Virtual.Lab

When the test runs were conducted in the NATC (Nevada Automotive Test Center), a trailer was attached to the HMMWV. Figure 2-5 shows a picture of the trailer

(a) and a Pro-E model of the trailer (b). The hardpoints gathered were for that trailer and in an attempt to increase the accuracy of the model, a trailer model was added to the existing HMMWV model.
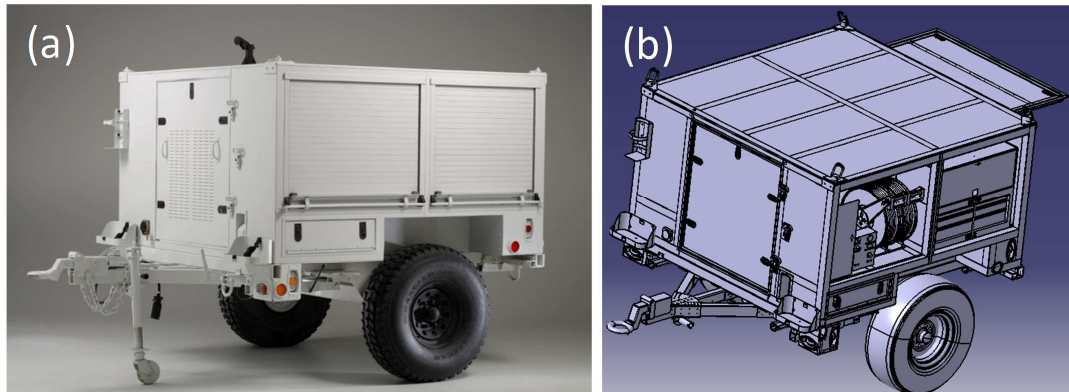
Figure 2-5: Trailer (a) LTT Common 22 Shop Set Trailer (source: www.schuttindustries.com) (b) Pro-E model of the Trailer

A suspension system for the trailer was created for simulation in Virtual.Lab. Six bodies were added to the HMMWV model. Table 2-3 shows the parts that were added to the model and Figure 2-6 shows the trailer suspension topology. The suspension system was modeled by adding a Rotational Spring Damper Actuator (RSDA) force element to the revolute joint between the A-arm and the Trailer Chassis. The spring constant was derived from an FE analysis that was simulated to match the trailer suspension system. The center of gravity of the trailer chassis was adjusted to match the trailer and the weight of the fully loaded trailer was added to the trailer chassis. An accurate Pro-Engineering CAD model was used to get the location of the center of gravity. The compete HMMWV-trailer model consisted of 71 bodies and can be seen in Figure 2-7.

Table 2-3: Trailer Topology Body Numbering

Body Number	Part Name
1	Lunette
2	Trailer Chassis
3	Left A-Arm
4	Right A-Arm
5	Left Trailer Wheel
6	Right Trailer Wheel

Figure 2-6: Trailer Suspension Topology

Figure 2-7: HMMWV-trailer Model in Virtual.Lab

CHAPTER 3

ROAD ELEMENT

3.1 Road profile introduction

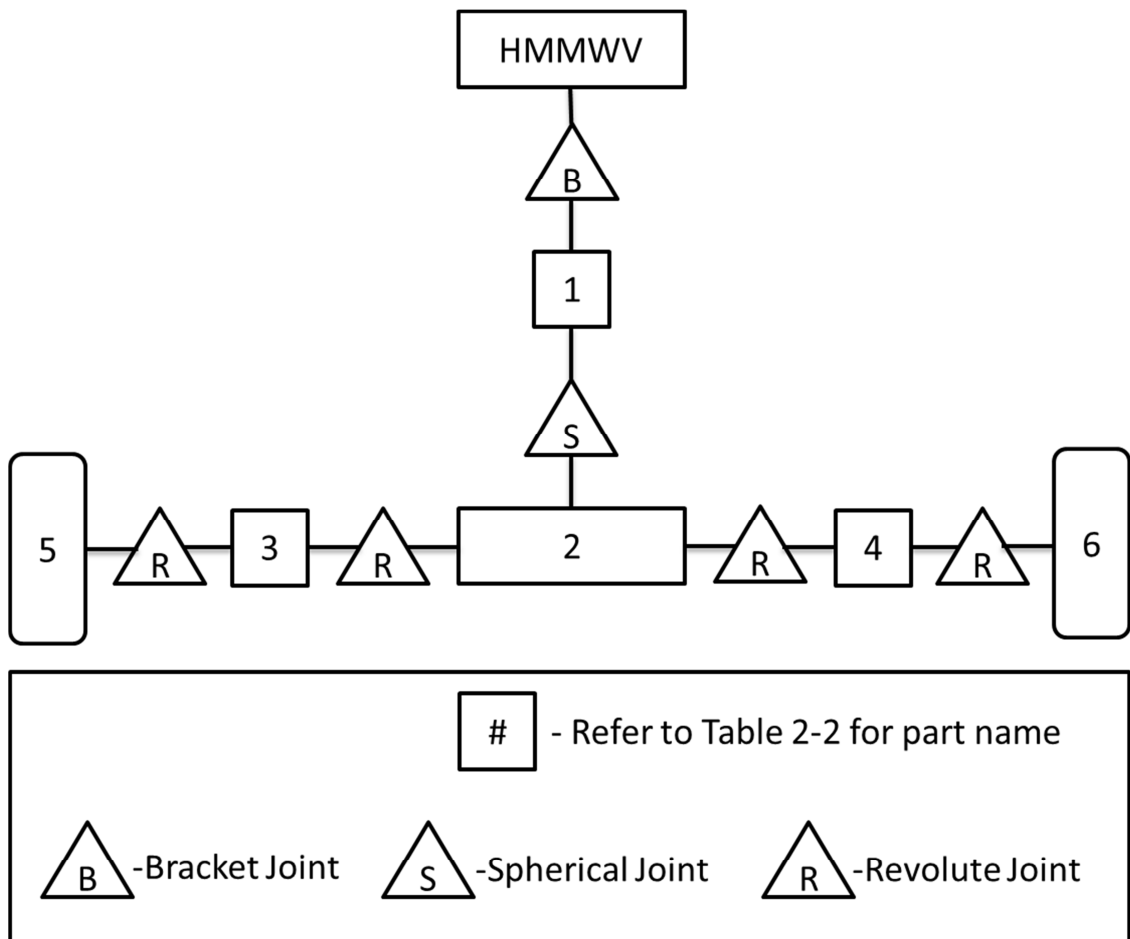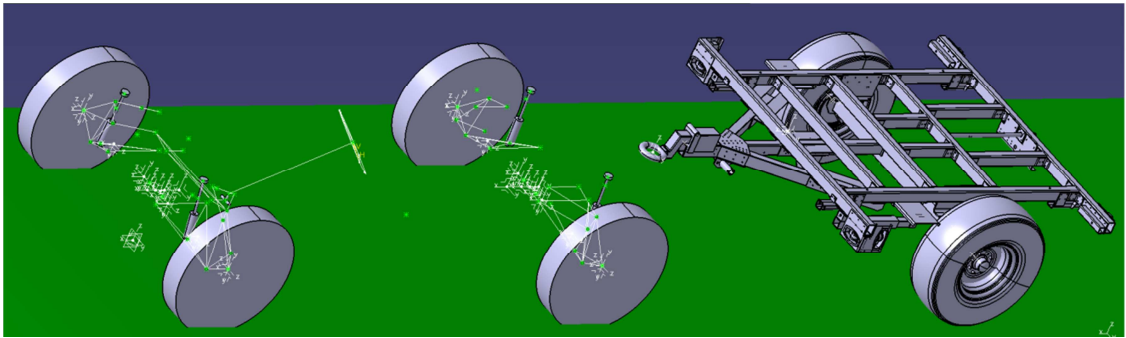Road profile data were taken, for example, by inertial profilers that use laser or ultrasonic systems because they provide fast and accurate readings of the road profile. However, even though the sampling rates of modern profilers are fast, the data taken are approximations to true profile of the road. It is possible to increase the sampling rate but the data collected will fill the storage space quickly. This is the reason that lower sampling rates are used and uncertainty to the road profile measurements needs to be ascertained. Some of the usage for road profiles includes monitoring the condition of a road network for pavement management systems, evaluating quality of newly constructed or repaired section, diagnosing the condition of specific sites and to using them as inputs to vehicle simulation models.

The road-tire interaction is one of the main inputs to the vehicle model. The roughness of the road defines how much vibration the vehicle is subjected to. The road profile used in the HMMWV model was data taken from the National Advanced Driving Simulator (NADS) database at The University of Iowa. The road data represents road roughness from test grounds found at the Aberdeen Proving Grounds in Maryland. The HMMWV-trailer tests conducted at NATC included driving on a rough test course, the Embedded Rock (NATC, 2010). The vehicle dynamics results from this test were used to validate the models presented in this thesis. The Embedded Rock course maintained by NATC was to match the road roughness of a corresponding test course at the Army's Aberdeen Proving Grounds. The road profile data of the Embedded Rock course

provided by NADS was gathered for only 100 m of the test course. To extend the

available road profile, a distribution function based methodology was created. The

original road profile was decomposed to extract the road parameters that defined the road

profile and selected distribution functions were tested to fit to the roughness parameters

that were used to specify road profiles beyond the 100-m range while the same roughness

parameters were maintained. The road profile provided by NADS resembles series of

square waves with various frequencies and magnitudes. Virtual.Lab allows for a spline

curve or a spline surface as input for road profiles. All of the road profiles used in this

study were entered as spline curves. Figure 3-1 shows how the square waves in the

spline curves are treated as road profiles. The left and the right side tires each have their

own road profile that they are following, thus each side has a different road profile.

Figure 3- 1: Sample Road Profile from Virtual.Lab

3.2 Procedure to calculate distribution

The road profile used in the simulation was characterized by three parameters: the roughness height of the road, the roughness interval, and the length of the roughness in each bump or square wave. In order to best match the given road profile, the road data were dissected to determine the three parameters described above. Figure 3-2 shows how the square wave was decomposed into the road parameters: roughness height, roughness length and roughness interval.
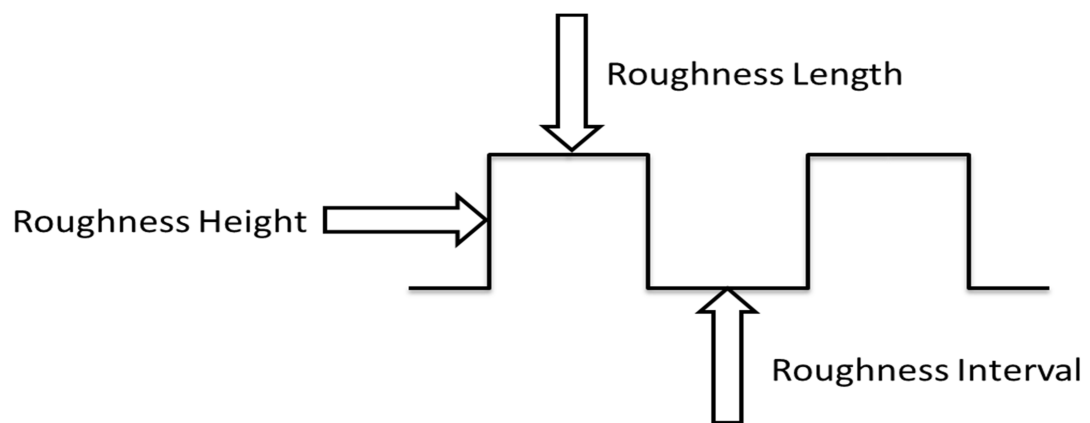
Figure 3- 2: Decomposition of Road Parameters

A statistical software, EasyFit (Math Wave, 2010), was used to find the best fitting distribution functions for each of the three road parameters. 700 data points for each of the parameters were extracted from the original road profile. EasyFit software uses a maximum likelihood estimation to fit the distribution function to the data. The goodness of fit was calculated by the software according to the Kolmogorov-Smirnov (K-S) test (MathWave, 2010). The K-S test is used to decide if a sample comes from a

specific distribution. It is based on the empirical cumulative distribution function

(ECDF). Given n ordered data points $y_1, y_2, \dots y_n$, the ECDF is defined as

$$F_n(y) = \frac{n(i)}{n} \qquad (3\text{-}1)$$

where $n(i)$ is the number of points less than y_i and y_i are ordered from smallest to largest

value. This is a step function that increases by n^{-1} at the value of each ordered data point.

(Engineering Statistics Handbook, 2011).

The K-S statistic (D) is based on the largest vertical difference between the

theoretical and the ECDF and is defined as

$$D = \max_{1 \le i \le n} \left((F_n(y_i) - \frac{i-1}{n}, \frac{i}{n} - F_n(y_i)) \right) \qquad (3\text{-}2)$$

where F is the theoretical cumulative distribution of the distribution being tested and max

is the maximum operator for $1 \le i \le n$ (Engineering Statistics Handbook, 2011).

A summary of the K-S test for best fit distributions for roughness height is listed

in Table 3-1, in which the results of 3 probability density functions (PDF) were given.

The low K-S values represent better fit to the data examined. Among the distribution

functions examined, a Frechet distribution was the best fit. The mathematical expression

for the PDF of Frechet distribution is given in Equation (3-3). Figure 3-3 shows the PDF

of Frechet distribution over the histogram of the roughness height data.

$$f(x) = \frac{\alpha}{\beta} \left(\frac{\beta}{x-\tau} \right)^{\alpha+1} \exp\left(-\left(\frac{\beta}{x-\tau} \right)^{\alpha} \right) \qquad (3\text{-}3)$$

where α and β are the continuous shape parameter, τ is the continuous location parameter

and x is a continuous random variable.

Figure 3-4 shows the Gamma distribution with the PDF given in Equation (3-4)

$$f(x) = \frac{x^{\alpha-1}}{\beta^{\alpha}\,\Gamma(\alpha)}\,\exp\left(-\frac{x}{\beta}\right) \tag{3-4}$$

where Γ is the Gamma function. Figure 3-5 shows the Inverse Gaussian distribution with the PDF given in Equation (3-5)

$$f(x) = \sqrt{\frac{\eta}{2\,\pi\,(x-\tau)^3}}\,\exp\left(-\frac{\eta(x-\tau-\mu)^2}{2\,\mu^2(x-\tau)}\right) \tag{3-5}$$

where η and μ are continuous parameters. Even when looking at the best fitting distribution for roughness height, the distribution function is not able to accurately capture the coarser roughness values. From looking at Figure 3-3 it is clearly seen that the Frechet distribution function only provides a good description of the peak value of around 0.25 in but fails to capture the higher roughness values of around 0.75 in. However, as mentioned earlier, the Frechet distribution is the best fit for the roughness height data.

Table 3-1: Goodness of Fit Summary For
Road Roughness Height

Distribution	K-S Statistic
Frechet	0.17783
Gamma	0.19701
Inv. Gaussian	0.20466
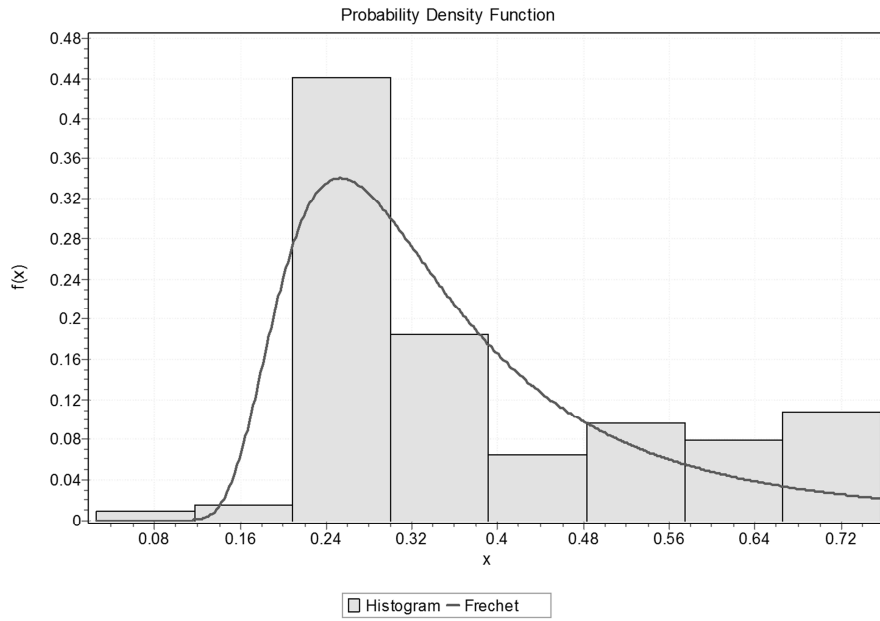
Figure 3-3: Frechet Distribution for Roughness Height
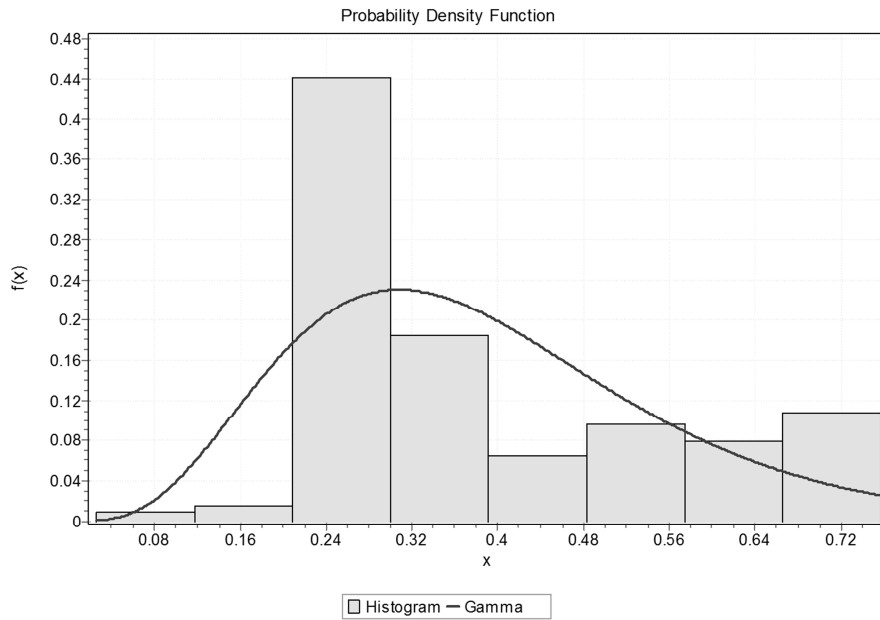
Figure 3-4: Gamma Distribution for Roughness Height
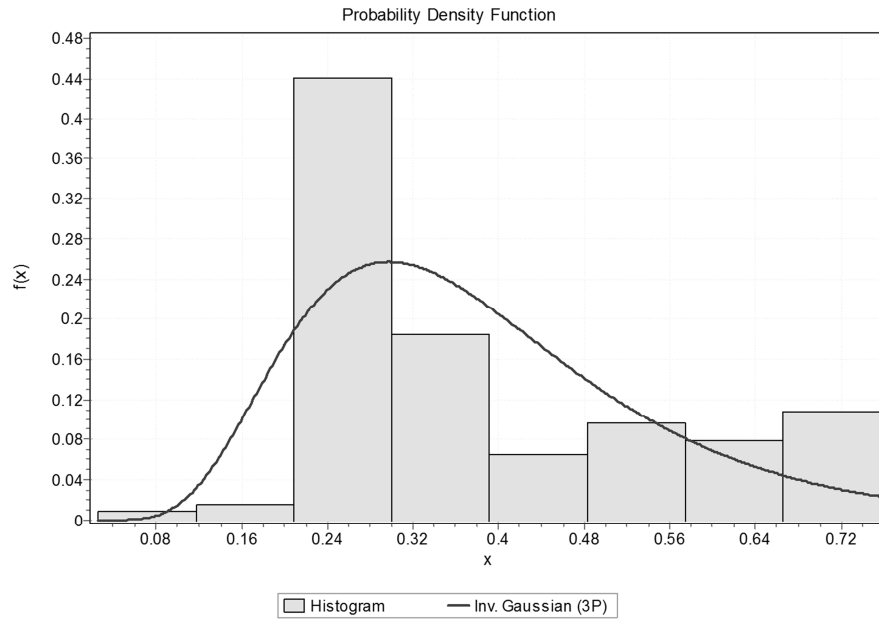
Figure 3-5: Inv. Gaussian Distribution for Roughness Height

For roughness intervals, three best fit distributions were the four Parameter Generalized Gamma (Gen. Gamma (4P)), four Parameter Person 6 (Person 6 (4P)), and Wakeby. Table 3-2 lists the K-S statistics for best fit distribution for roughness interval. Figure 3-6 shows the Gen. Gamma (4P) distribution, which is the best fit for the roughness interval and its PDF is listed in Equation (3-6)

$$f(x) = \frac{k(x-\tau)^{k\alpha-1}}{\beta^{k\alpha}\ \Gamma(\alpha)} \exp\left(-\left(\frac{x-\tau}{\beta}\right)^k\right) \tag{3-6}$$

where k is a continuous shape parameter.

Figure 3-7 shows the Person 6 (4P) distribution with the PDF listed in Equation (3-7)

$$f(x) = \frac{(\frac{x-\tau}{\beta})^{\alpha_1-1}}{\beta\ B(\alpha_1,\alpha_2)\left(1+\frac{x-\tau}{\beta}\right)^{\alpha_1+\alpha_2}} \tag{3-7}$$

where B is the beta function and α_1 and α_2 are continuous shape parameters. Figure 3-8

shows the Wakeby distribution and the inverse cumulative distribution function (ICDF)

listed in Equation (3-8)

$$F(x) = \xi + \frac{\alpha}{\beta}(1 - (1 - x)^\beta - \frac{\tau}{\delta}(1 - (1 - x)^{-\delta}) \tag{3-8}$$

where ξ and δ are all continuous parameters. The Wakeby PDF is numerically evaluated

as a derivative of the cumulative distribution function, which in turn is calculated based

on the ICDF.

All three distributions for roughness interval provide a good fit for the data and

can be seen from the very low K-S statistics. The three K-S statistics on Table 3-2 are

relatively close to each other which also signify that any of the three distributions would

produce accurate description of the roughness interval.

Table 3-2: Goodness of Fit Summary
for Roughness Interval

Distribution	K-S Statistic
Gen. Gamma (4P)	0.02543
Pearson 6 (4P)	0.02669
Wakeby	0.02757
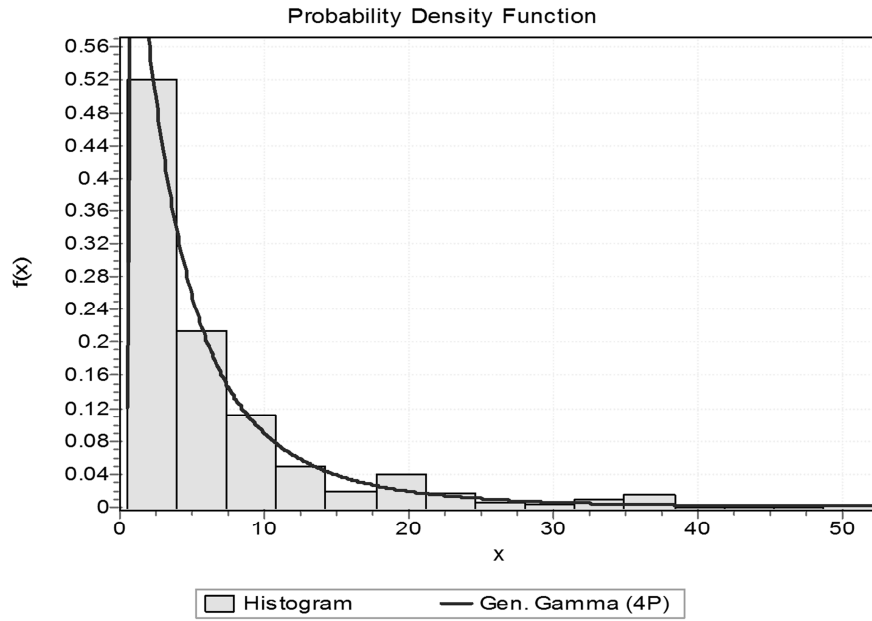
Figure 3-6: Gen. Gamma Distribution for Roughness Interval
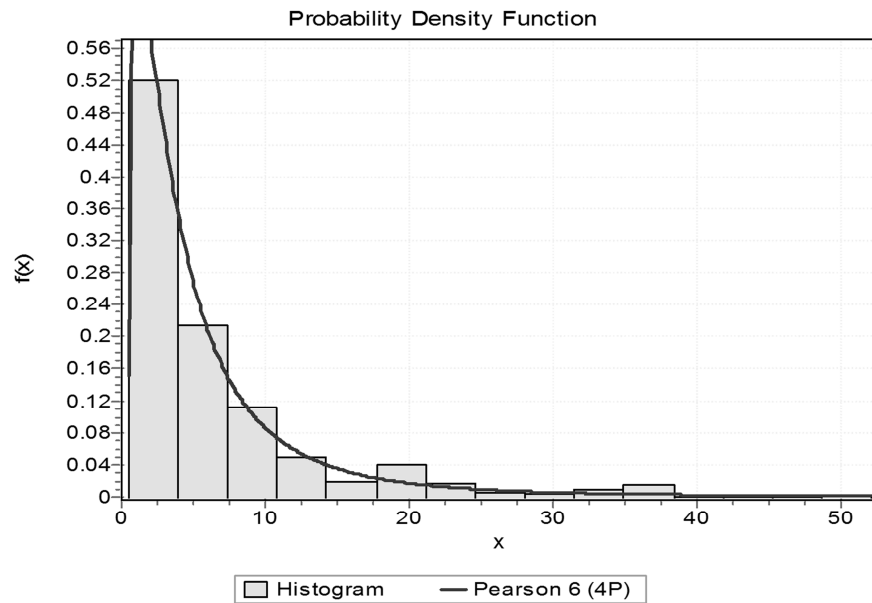
Figure 3-7: Pearson 6 Distribution for Roughness Interval
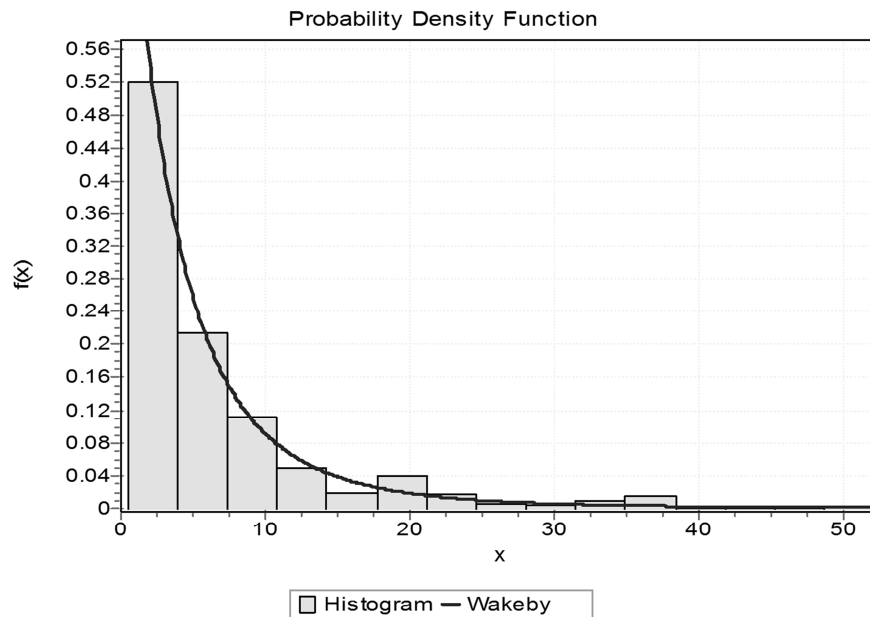
Figure 3-8: Wakeby Distribution for Roughness Interval

Table 3-3 lists the K-S statistics for best fit distribution for roughness length. The three best fit distributions were Wakeby, three parameter Lognormal (Lognormal (3P)), and three parameter Gamma distribution (Gamma distribution (3P)). Low values of the K-S statistics for all three distributions again represent that they provide a good description for the roughness length data. Any of the distributions in Table 3-3 are statistically adequate to represent the roughness length. Figures 3-9 shows the Wakeby distribution which was the best fit distribution according to the K-S Statistic. Figure 3-10 shows the Lognormal (3P) distribution and Equation (3-9) shows its PDF.

$$f(x) = \frac{\exp\left(-\frac{1}{2}\left(\frac{\ln(x-\tau)-\mu}{\sigma}\right)^2\right)}{(x-\tau)\sigma\sqrt{2\pi}}$$ (3-9)

Finally Figure 3-11 shows the Gamma distribution (3P) fit over the histogram of the roughness length data. Equation (3-10) shows the PDF for Gamma Distribution (3P).

$$f(x) = \frac{(x-\tau)^{\alpha-1}}{\beta^{\alpha}\Gamma(\alpha)} exp\left(-\frac{x-\tau}{\beta}\right) \qquad (3\text{-}10)$$

After looking at all three distributions, it can clearly be seen that the Wakeby

distribution function in Figure 3-9 does the best in describing the peak value of around

0.45 in. This is again represented by the lowest K-S value in Table 3-3.

Table 3-3: Goodness of Fit
Summary for Roughness Length

Distribution	K-S Statistic
Wakeby	0.0544
Lognormal (3P)	0.05998
Gamma (3P)	0.06164

Figure 3-9: Wakeby Distribution for Roughness Length

Figure 3-10: Lognormal Distribution for Roughness Length

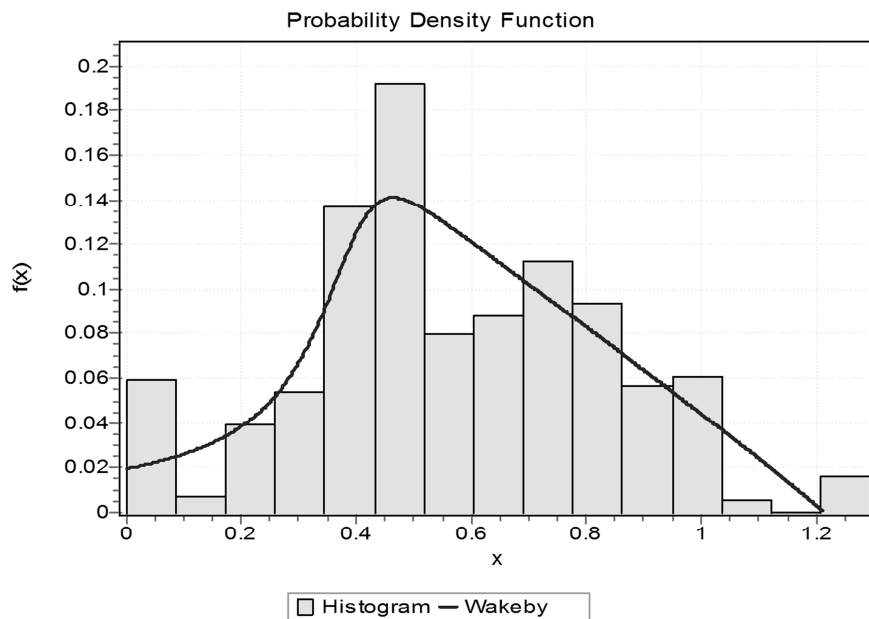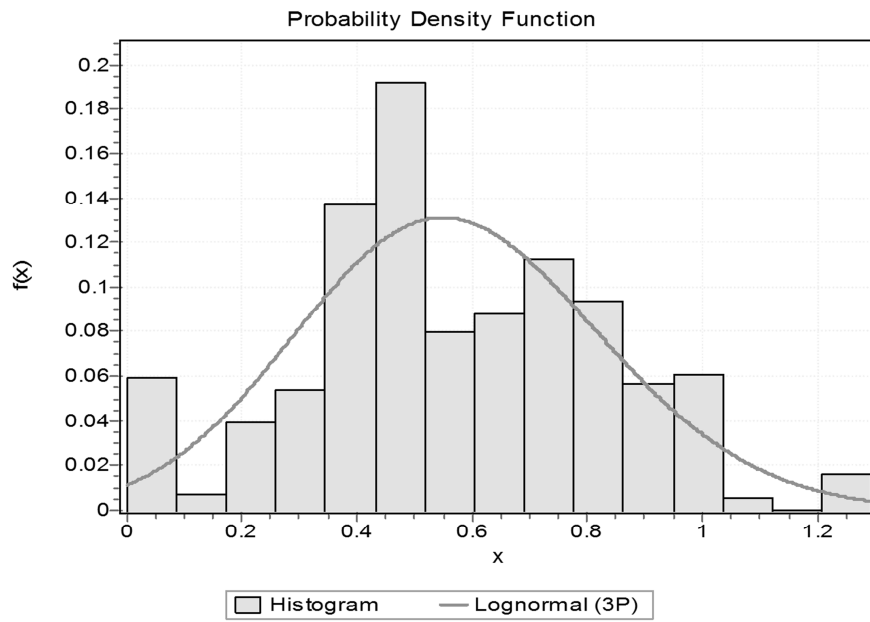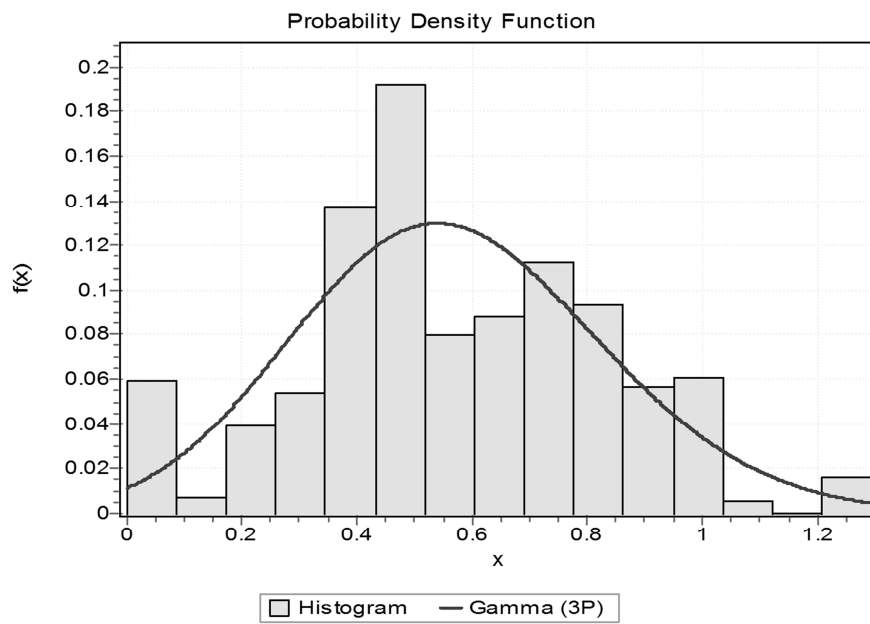Figure 3-11: Gamma Distribution for Roughness Length

The results of K-S tests suggest that distribution functions were adequate to describe the roughness length and interval of road profile data examined. However, distribution functions examined were not adequate to describe the roughness height. According to Rouillard et al. (2001), the majority of the roughness should be described by an offset Rayleigh distribution function; whereas Bogsjo (2006) stated that the general roughness of the road was described by a Gaussian distribution. Since the length of the road that was used to derive the distribution for the road roughness was only around 100 m and only 700 data points were extracted from the original road profile, there were not enough data points to see similarities with the findings of Rouillard (2001) and Bogsjo (2006).

The best fitting distribution functions that describe the roughness height, interval and length of the bumps were used to generate random numbers. Frechet distribution was used for roughness height, while Gen. Gamma (4P) distribution was used for roughness length and Wakeby distribution was used for the roughness interval. Every single random number generated from the three distributions correlates to a single bump on the road profile. The length of the road is only limited by the number of random numbers generated using the distribution. A Mathematica (Wolfram, 2008) code was written to compile the sets of random numbers to generate a road profile, see Appendix A. Figures 3-12 show a sample of the original road profile data and the generated road profile from the distribution functions. The generated road profile is able capture the key trends like the high roughness value of around 0.7 in and the lower roughness values between 0.25 and 0.4 in. Roughness length and interval is also accurately generated as can be seen by the comparable width and interval between each of the square waves.
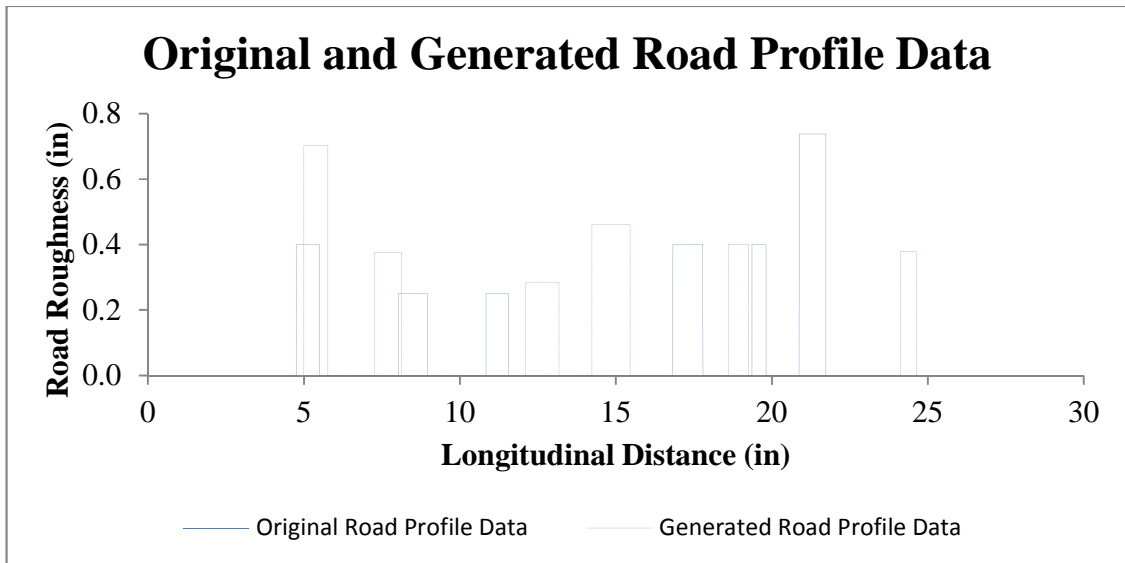
Figure 3-12: Example of the Original and Generated Road Profile

3.3 Updated model validation

To validate this method to create the road profile and the updates made to the

HMMWV and trailer model, the model was first tested using the original road profile and

then solved using the road profile generated with the distributions (new road profile).

The results from the simulations were then compared with dynamic test results.

Measurements that Zeman (2009) solved for included the RMS, maximum, and minimum

acceleration values. Similar measurements were extracted from the two simulations and

compared with the dynamic test results. Data were recorded at the driver seat for all

three components of acceleration. In simulation, a dummy body was attached to the

chassis at the location of the driver seat to extract acceleration data from this location.

First the updated HMMWV model was tested using the original road profile.

Table 3-4 shows the driver vertical acceleration results for the original road profile. The

low relative error compared to the dynamic tests signifies that the model captures the

vertical acceleration characteristics well. Table 3-5 shows the vertical acceleration data for the original road profile from the old model (Zeman, 2009). The results for the driver vertical acceleration can be found in Figure 3-13 for the updated model and Figure 3-14 shows the results obtained by Zeman with the original model (Zeman, 2009). The RMS value for the updated HMMWV model, listed in Table 3-4, shows that the model is able to accurately capture the RMS values of the dynamic tests to the first decimal place. The error in the second decimal place is attributed to simulation and road profile errors and uncertainty in the measurements. When comparing the results from the updated model to the results from the old model in Table 3-5, the RMS value is lower than what was previously observed. Results from the updated model are closer to the dynamic test 1 while the results from the old model are closer to the dynamic test 2 results. This can be seen by the distribution of the relative errors between the two tests and shows that the RMS value is still accurately captured by the updated model. The maximum acceleration is also captured accurately by the model as seen by the low relative errors. The updated model under-estimates the maximum acceleration compared to the old model, which has acceleration values between the two dynamic test results. Minimum acceleration is also under predicted by the updated model compared to the old model but the acceleration values fall below the two dynamic test results. This increase in the error in the minimum acceleration was caused by the updates made to the model. There is large variability observed between the dynamic test results for maximum and minimum acceleration as seen in Tables 3-4 and 3-5. It should also be noted that the RMS of the acceleration value is the more important measurement for vehicle simulation and the updated model captures it well.

Table 3- 4: Vertical Acceleration Data for Updated Model with Original Road Profile

Test Condition	RMS Acceleration(g)	Maximum (Acceleration(g)	Minimum Acceleration(g)
Updated HMMWV Model	0.24	1.16	-1.35
Dynamic Test 1	0.23	1.12	-1.53
Relative Error	2.5%	3.5%	11.6%
Dynamic Test 2	0.26	1.30	-1.73
Relative Error	9.1%	10.8%	21.9%

Table 3-5: Vertical Acceleration Data for Old Model with Original Road Profile (Zeman, 2009)

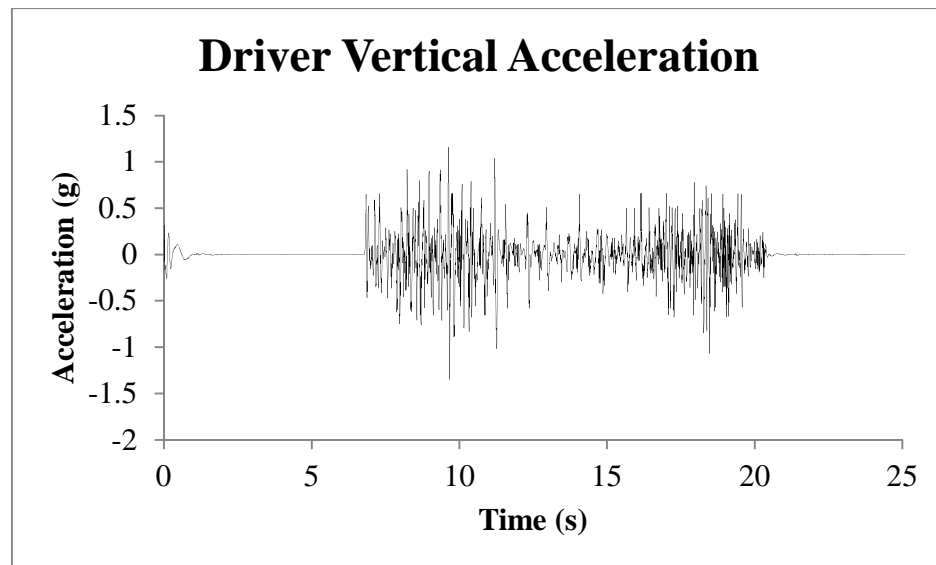| Test Condition	RMS Acceleration(g)	Maximum (Acceleration(g)	Minimum Acceleration(g)
Old HMMWV Model	0.25	1.32	-1.61
Dynamic Test 1	.23	1.12	-1.53
Relative Error	7.6%	17.2%	4.9%
Dynamic Test 2	0.26	1.30	-1.73
Relative Error	4.53%	1.7%	6.95%

Figure 3-13: Driver Vertical Acceleration for Updated Model
with Original Road Profile
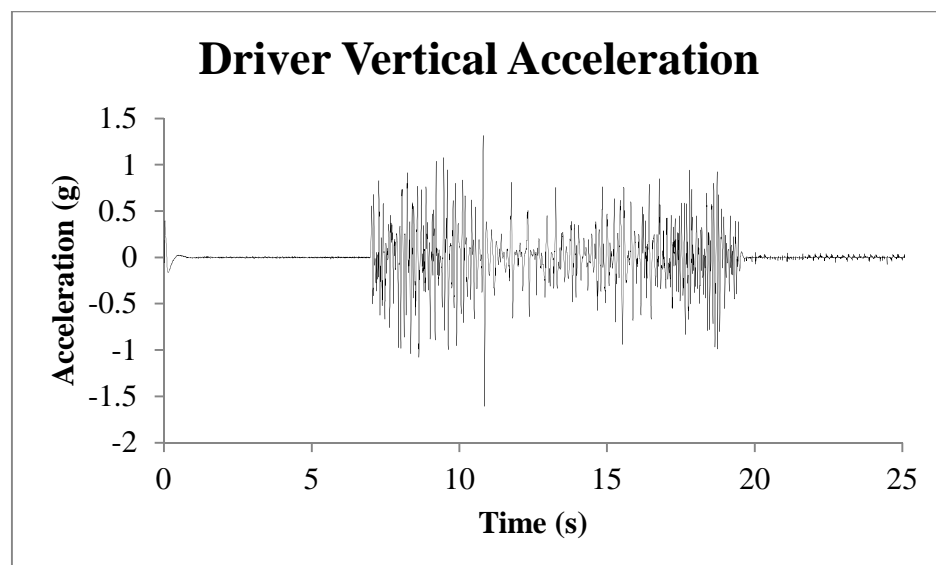
Figure 3-14: Driver Vertical Acceleration for Original Model
with Original Road Profile (Zeman, 2009)

3.4 Road profile methodology validation

In order to validate the road profiles created from the distribution functions, the results from updated model using the new road profile were compared to the results from the original road profile. The new road profiles are not unique because of the random numbers generated for the road parameters. In order to study how the simulation results vary from using different road profiles that are generated from the same distribution function and the effect of changing simulation length, series of tests were conducted. These tests include multiple road profiles that were run for different simulation lengths. The road profiles were generated using the best fitting distributions and a different road profile was created for each simulation length tested. Table 3-6 shows the RMS of the vertical acceleration for the test runs. Simulation lengths were varied from 30, 60, 120, 240 and 480 seconds. The results are plotted in a semi-log plot in Figure 3-15. The linear trend shown in the figure reflects that the RMS is not influenced by changing road or different simulation length. Since the RMS value stays constant with respect to time, only one value from a 60 sec simulation, using the new road profile, was taken to compare with the results from the original road profile.

Table 3-6: RMS of Driver Vertical Acceleration for
Test Runs

Road Profile	RMS (g)	Simulation Length (sec)
Profile 1	.209	30
Profile 2	.210	60
Profile 3	.209	120
Profile 4	.210	240
Profile 5	.212	480
Profile 6	.212	960
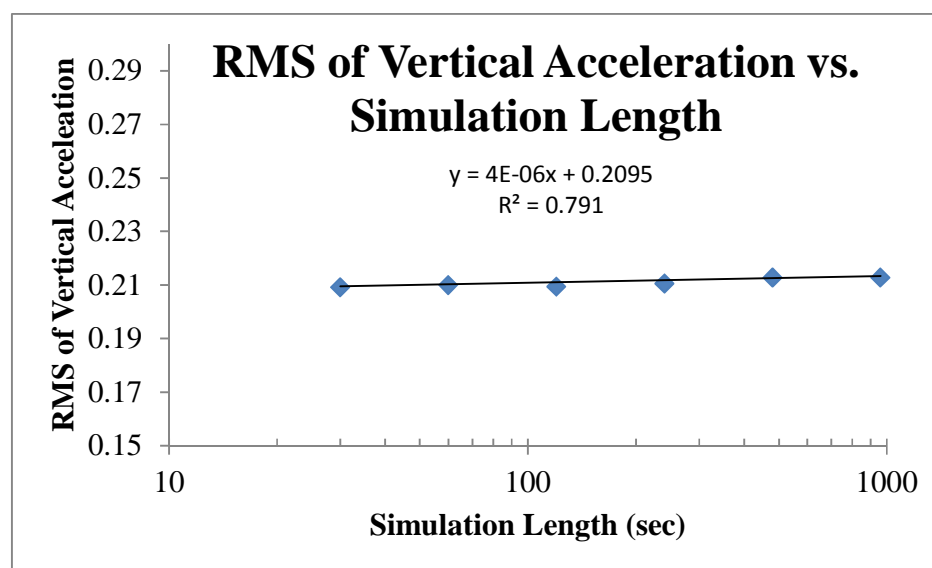
Figure 3-15: RMS-Vertical Acceleration vs. Simulation Length

Table 3-7 shows the vertical acceleration results from the updated model using the new road profile. Figure 3-16 shows the driver vertical acceleration for the updated model using the new road profile. Driver vertical acceleration for dynamic test 1 is shown in Figure 3-17. The model is again able to predict the RMS value accurately to the first decimal place. The maximum acceleration result from the new road profile is very close the dynamic test 1seen from the low relative error but has more relative error when compared to dynamic test 2. The model does not predict the minimum acceleration well when using well when using the new road profile. Overall, the model under-predicts the vertical acceleration compared to results from Table 3-4 for the original road profile. This can also be seen when comparing Figure 3-16 and 3-17. The under-prediction amplifies the minimum acceleration because of the updates made to the model. However it should be noted that both maximum and minimal acceleration is highly sensitive to the

high roughness values and can be misleading because of one outlying value. The under-prediction of the acceleration results is due to the low number of data points used to fit the distribution. As discussed earlier, Figure 3-3 shows how the Frechet distribution, used to generate the roughness height data, does a good job of describing the roughness data of the of peak values for lower roughness value. The distribution however does not accurately describe the higher roughness values and thus does not generate enough higher roughness values for the road profile. The lower number of high roughness values compared to the original road profile translates to lower vertical acceleration values predicted by the model seen in Table 3-7. If more data points were used to fit the distribution functions, then the distribution functions would better describe the roughness data and thus improve the results from the model. Even with the overall lower acceleration values, the new road profile has shown to produce RMS values that is within 0.03 g of the results from the original road profile. It should also be noted that the uncertainty of simulation is much tighter than dynamic test results shown by the low random error and with more data points to fit the distributions the results could improve even more. With this, the methodology for creating road profiles using distribution function was validated.

Table 3- 7: Vertical Acceleration Data for Updated Model with New Road Profile

Test Condition	RMS Acceleration(g)	Maximum (Acceleration(g)	Minimum Acceleration(g)
Updated HMMWV Model	0.21	1.10	-1.14
Dynamic Test 1	0.23	1.12	-1.53
Relative Error	8.4%	2.0%	25.3%
Dynamic Test 2	0.26	1.30	-1.73
Relative Error	18.8%	15.6%	33.9%

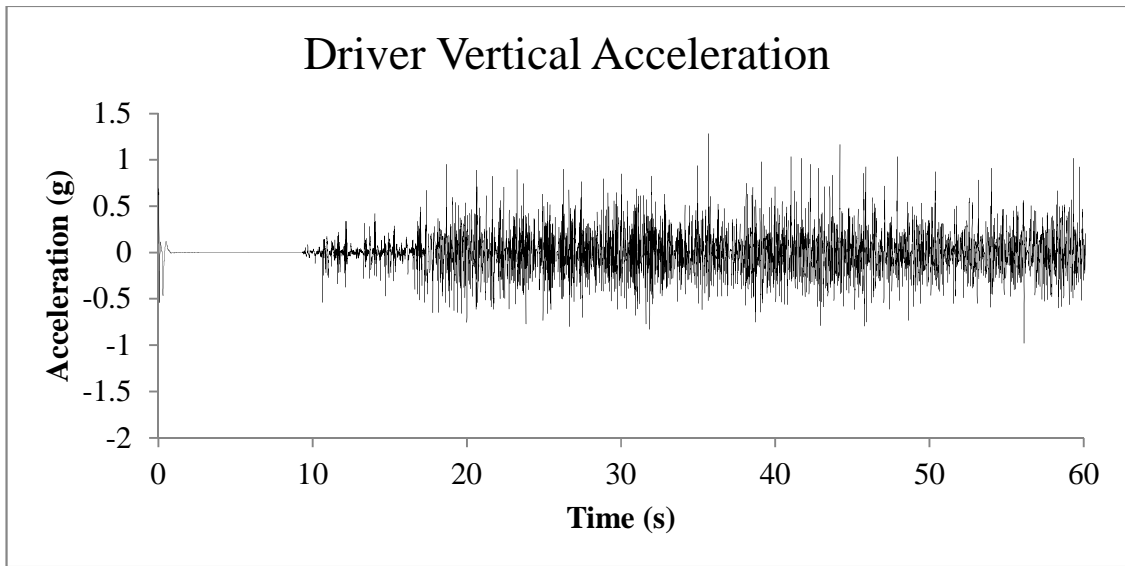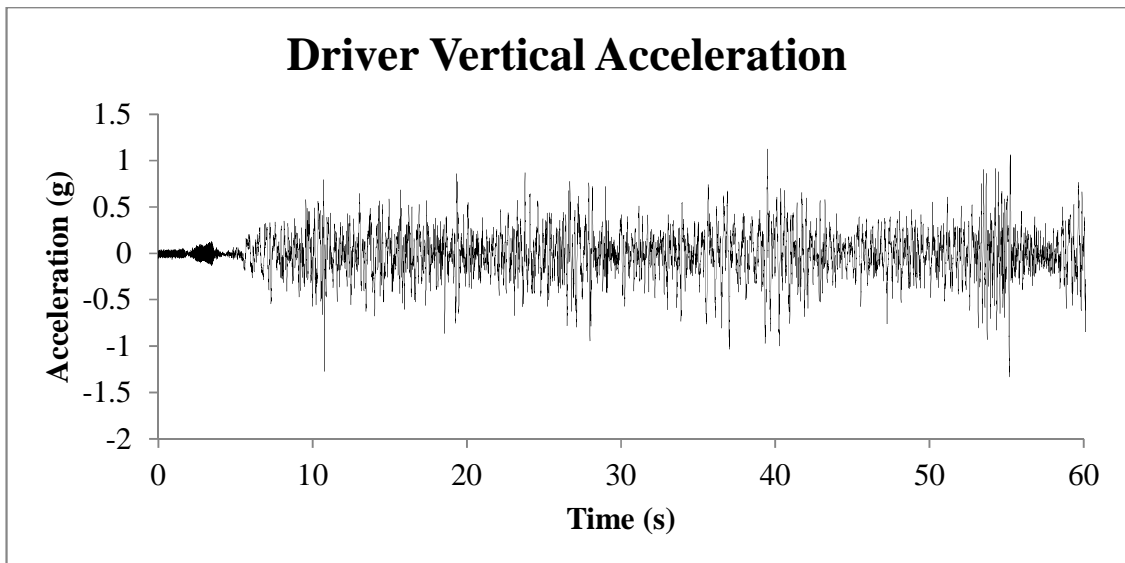Figure 3-16: Driver Vertical Acceleration for Updated Model with New Road Profile

Figure 3-17: Driver Vertical Acceleration from NATC Data

Table 3-8 shows the longitudinal acceleration data for the updated model on the original road profile. The longitudinal results are very similar to Table 3-9 which shows the longitudinal acceleration data for the old model on the original road profile (Zeman,

2009). Only slight improvements were observed with the updated model seen by slightly lower relative errors for maximum and minimum accelerations. Table 3-10 shows the longitudinal results for the updated model on the new road profile and because of the overall lower acceleration prediction, the relative errors from this simulation were significantly less than results from the original road profile. This shows that the longitudinal is very sensitive to the roughness of the road profile. The trailer added to the HMMWV model was a basic model and more refinement needs to be made before significant improvements to the longitudinal acceleration can be expected. Even though improvements in longitudinal were not observed, the updated model was validated for vertical direction and the methodology for creating road profiles from distribution was also validated. Utilizing these two components, the updated model and the road profiles, a parametric study was conducted to study the effects of road variability on vehicle models.

Table 3- 8: Longitudinal Acceleration Data for Updated Model with
Original Road Profile

Test Condition	RMS Acceleration(g)	Maximum (Acceleration(g)	Minimum Acceleration(g)
Updated HMMWV Model	0.17	0.81	-1.31
Dynamic Test 1	0.10	0.46	-0.84
Relative Error	63.5%	73.7%	55.8
Dynamic Test 2	0.12	0.48	-1.39
Relative Error	42.7	67.5	5.4%

Table 3- 9: Longitudinal Acceleration Data from Original Simulation (Zeman, 2009)

Test Condition	RMS Acceleration(g)	Maximum Acceleration(g)	Minimum Acceleration(g)
Old HMMWV Model	0.17	0.89	-1.02
Dynamic Test 1	0.10	0.46	-0.84
Relative Error	63.1%	92.0%	20.8%
Dynamic Test 2	0.12	0.48	-1.39
Relative Error	42.4%	85.3%	26.6%

Table 3- 10: Longitudinal Acceleration Data for Updated Model with New Road Profile

Test Condition	RMS Acceleration(g)	Maximum (Acceleration(g)	Minimum Acceleration(g)
Updated HMMWV Model	0.13	0.67	-0.91
Dynamic Test 1	0.10	0.46	-0.84
Relative Error	28.2%	44.9%	7.6%
Dynamic Test 2	0.12	0.48	-1.39
Relative Error	11.9%	39.8%	34.6%

CHAPTER 4

PARAMETRIC STUDY

4.1   Road preparation

When creating a road profile that represents the road surface condition, the road

parameters describing the road profile should be captured accurately. Any error can have

an adverse effect on results from the vehicle model. To study how changes in the road

parameters affect the vehicle model, the parameters describing the distribution functions

were varied.

To conduct the parametric study, the Gamma distribution function was chosen to

generate the roughness height values. The advantage of using Gamma distribution

function over other distribution functions given in Table 3-1 is that closed form

representations of the mean and variance are readily available. The mathematical

equation of the Gamma distribution is defined by Equation (4-1):

$$f(x) = \frac{x^{\alpha-1}}{\beta^{\alpha} \, \Gamma(\alpha)} \exp(-\frac{x}{\beta}) \qquad\qquad (4\text{-}1)$$

Frechet distribution was the best fit distribution for roughness height, however, a

closed form representation of the mean and variance for Frechet distribution is not

available.   For this reason Gamma distribution will be used to describe the roughness

height for the parametric study. The defining parameters (α and β) of the Gamma

distribution can be calculated directly by using the mean and the variance of the desired

roughness value. Equation (4-2) and (4-3) shows how the mean and the variance is

calculated from α and β, respectively; which in term depict the specific shape of the

Gamma distribution.

$$\bar{x} = \alpha \cdot \beta \qquad\qquad (4\text{-}2)$$

$$Var(x) = \alpha \cdot \beta^2 \qquad\qquad (4\text{-}3)$$

This property makes the Gamma distribution easy to use in the parametric study because variation of the road profile can be created by just varying the mean or the variance of the road roughness height. In this thesis, only the variation of roughness height was studied; the distribution functions describing the roughness length and interval were not changed.

Mean of the roughness height was varied from 1% change to 30%. Table 4-1 shows the increments of changes, the mean and variance values, and the α and β parameters used to define the Gamma distribution function in Equation (4-1). In Table 4-1 positive percent represent increase in the roughness (e.g. 10% represent 110% of mean value). Similarly negative percent represents decrease in the mean roughness value (e.g. -10% represents 90% of mean value). Fine increments of changes were taken to study when the changes made to the road profile began to affect the results predicted by the vehicle dynamics simulation. Microsoft Excel 2010 was used to generate the roughness values. An add-in feature for Excel from the Easy Fit software was used to generate the random numbers that fit the gamma distribution. Easy Fit uses the Mersenne Twister algorithm to generate pseudorandom numbers (L'Ecuyer, 2007). The pseudorandom number generator has a period of more than 10^{6000} numbers and passes numerous tests for statistical randomness (Math Wave, 2010).

Table 4-1: Gamma Distribution Parameters
for Small Variations in Mean Roughness

% Mean	$\bar{x}$	Var	α	β
30%	0.662	0.052	8.345	0.079
26%	0.642	0.052	7.839	0.081
22%	0.621	0.052	7.349	0.084
18%	0.601	0.052	6.875	0.087
14%	0.581	0.052	6.417	0.090
10%	0.560	0.052	5.974	0.093
8%	0.550	0.052	5.759	0.095
6%	0.540	0.052	5.548	0.097
4%	0.530	0.052	5.340	0.099
2%	0.519	0.052	5.137	0.101
1%	0.514	0.052	5.514	0.102
CTRL	0.509	0.052	4.937	0.103
-1%	0.504	0.052	4.839	0.104
-2%	0.499	0.052	4.742	0.105
-4%	0.489	0.052	4.550	0.107
-6%	0.479	0.052	4.363	0.109
-8%	0.469	0.052	4.179	0.112
-10%	0.458	0.052	3.999	0.114
-14%	0.438	0.052	3.652	0.120
-18%	0.418	0.052	3.320	0.125
-22%	0.397	0.052	3.004	0.132
-26%	0.377	0.052	2.704	0.139
-30%	0.356	0.052	2.419	0.147

Values for roughness interval were generated using the Generalized Gamma

distribution shown in Equation (3-6) and roughness length values were generated using

the Wakeby distribution function in Equation (3-8). All the values for the road profile

were generated using the pseudorandom number generator from Excel for the three

distributions. In order to complete one round of tests, twenty three road profiles were

created, one for each of the rows in Table 4-1.

4.2 Measurement

As referenced in Zeman (2009), RMS is a suitable criterion for quantifying the vertical acceleration experienced by the driver. RMS for the driver vertical acceleration will be used to compare the results from the different simulations. As the number of random numbers used to generate the road profiles increase, the chance of generating an outlying extreme value also increases. Maximum and minimum only reflect one value in the thousands of data points and are very sensitive to an extreme roughness. Since RMS is not affected by random extreme values, only the RMS of the driver vertical acceleration was analyzed.

4.3 Data analysis

Three sets of tests were completed with a total of sixty nine road profiles tested. The RMS values for the three test sets were averaged for each of the acceleration components. Figure 4-1 shows the percent change in mean roughness (PCMR) versus percent change in the RMS (PCRMS) value for vertical acceleration at the driver seat. Relative error between the control case RMS value and the observed RMS value for the various cases was defined as the percent change in the RMS. Given the control RMS value (CRMS) and the observed RMS value (ORMS), the PCRMS values was defined as

$$PCRMS = \frac{|CRMS - ORMS|}{|CRMS|} \times 100 \qquad (4\text{-}4)$$

From Figure 4-1 it can be seen that as the PCMR increases and decreases the RMS value also increases and decreases. The linear regression line shows a linear relationship between PCMR and PCRMS. The correlation of determination of $R^2 = 0.97$ indicates that 97% of the variance in PCRMS is accounted for by the fit. The standard error of the fit is defined as

$$S_{yx} = \sqrt{\frac{\sum_{i=1}^{N}(z_i - z_c)^2}{v}} \qquad (4\text{-}5)$$

where $v = N - (m+1)$, m = order of polynomial fit, and $(z_i - z)$ is the difference between the observed and predicted value from the polynomial fit. The error of the fit is related to how closely a polynomial fits the data set (Figliola et al., 2006). The error of fit for Figure 4-1 was $S_{yx} = 2.03\%$. These values suggest that a linear fit is a reliable relation between PCRM and PCRMS for vertical acceleration. Slope of 0.66 of the regression line indicates the sensitivity in that for every 1% change in PCRM there is 0.66% change in PCRMS.
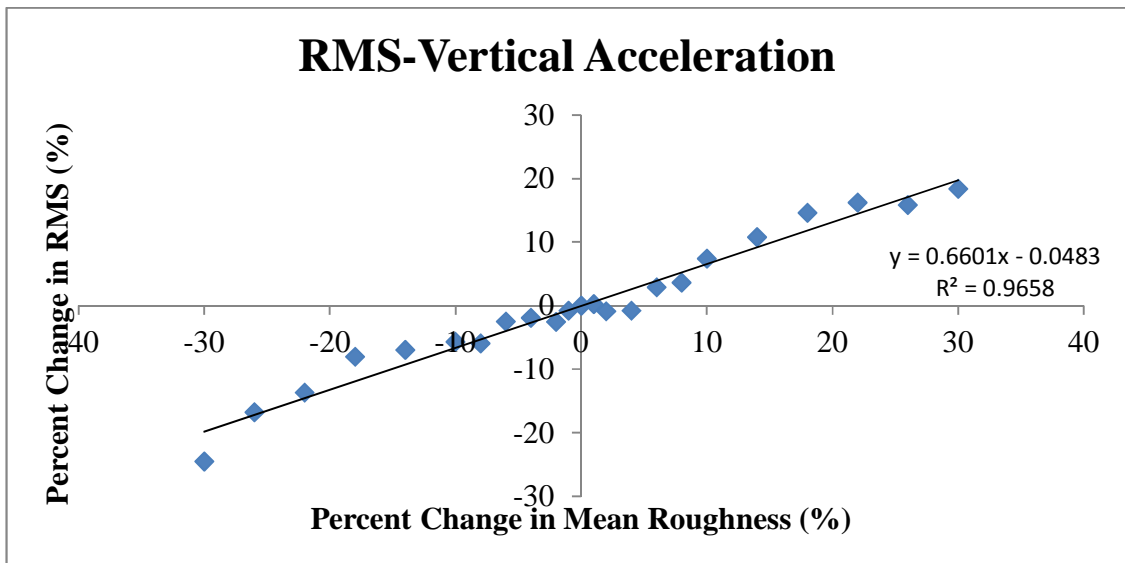

Figure 4-1: Change in RMS of Vertical Acceleration vs. Mean Roughness

Figure 4-2 shows the PCMR verses the PCRMS of the longitudinal acceleration at the driver's seat. The data points are grouped close to the linear trend line similar to Figure 4-1. The correlation of determination of $R^2 = 0.96$ indicates that 96% of the variance in PCRMS is accounted for by the fit. The error of fit for Figure 4-2 was $S_{yx} = 2.05\%$. These values suggest that a linear fit is again a reliable relation between PCRM and PCRMS for longitudinal acceleration. Slope of 0.64 for the trend line indicates that for every 1% change in PCRM there is 0.64% change in PCRMS for longitudinal acceleration.

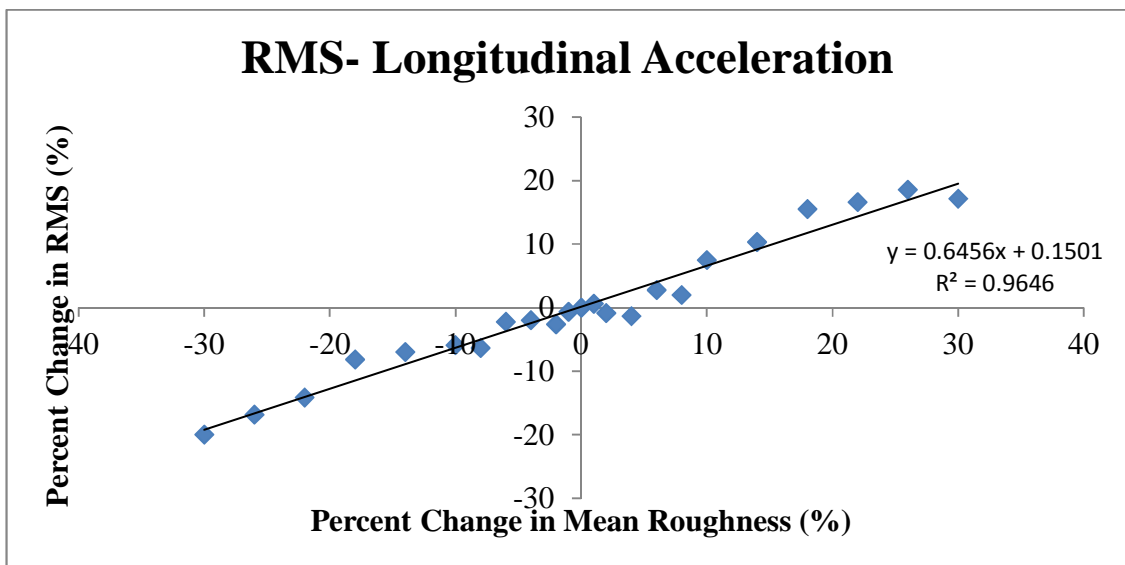Figure 4-2: Change in RMS of Longitudinal Acceleration vs. Mean Roughness

Figure 4-3 shows the PCMR verses the PCRMS of the lateral acceleration at the driver's seat. The data points are not grouped close to the linear trend line unlike Figure 4-1 and 4-2. The correlation of determination of $R^2 = 0.84$, suggesting linear-fit is less satisfactory for lateral acceleration than the normal and longitudinal acceleration. This

aspect is also reflected by the error of fit, $S_{yx} = 5.06\%$, which is significantly larger than

the previous two error of fit of vertical and longitudinal accelerations. These values

suggest that a linear fit is not as reliable relation between PCRM and PCRMS for lateral

acceleration. Even though the linear fit is not as reliable relation, the slope of 0.70 for the

trend line is comparable to the slopes for Figure 4-1 and 4-2. Slope of 0.7 indicates that

for every 1% change in PCRM there is 0.7% change in PCRMS for lateral acceleration.
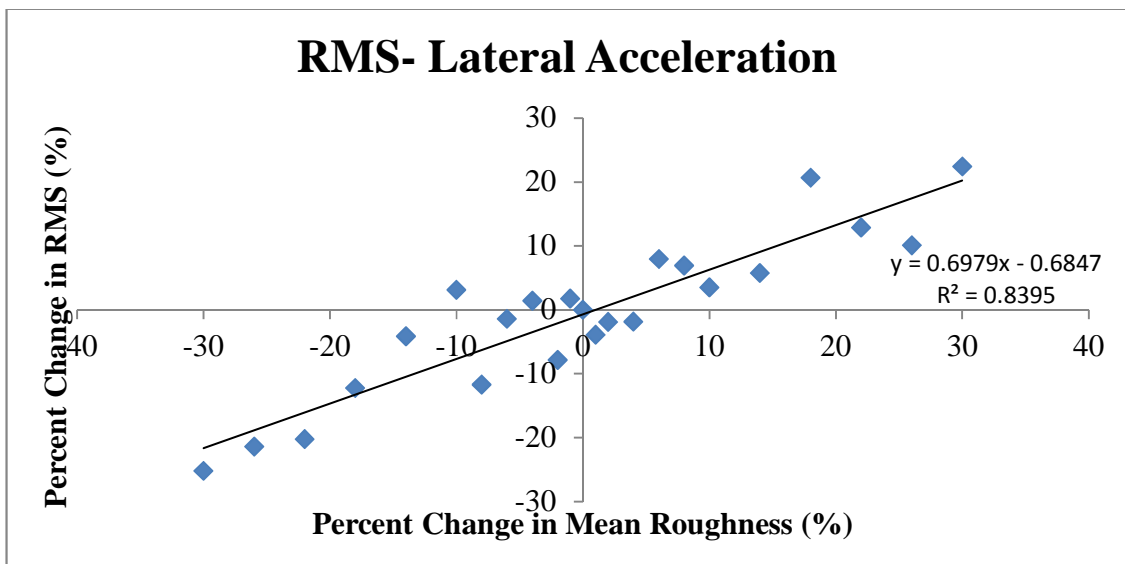

Figure 4-3: Change in RMS of Lateral Acceleration vs. Mean Roughness

For small percent change in the mean roughness (e.g., less than 40%) a linear

response is suggested by the results given in Figures 4-1 to 4-3. To examine whether or

not the linear trend continues for larger changes in the mean roughness, the variance was

extended to ±100% as summarized in Table 4-2.

Table 4-2: Gamma Distribution Parameters
for Large Variations in Mean Roughness

%Mean	$\bar{x}$	Var	α	β
100%	1.020	0.053	19.752	0.052
80%	0.918	0.053	15.999	0.057
40%	0.714	0.053	9.679	0.074
20%	0.612	0.053	7.111	0.086
10%	0.561	0.053	5.975	0.094
5%	0.535	0.053	5.444	0.098
CTRL	0.510	0.053	4.938	0.103
-5%	0.484	0.053	4.457	0.109
-10%	0.459	0.053	4.000	0.115
-20%	0.408	0.053	3.160	0.129
-60%	0.204	0.053	0.790	0.258
-80%	0.102	0.053	0.198	0.516
-90%	0.051	0.053	0.049	1.032

Figure 4-4, 4-5 and 4-6 shows the PCMR versus PCRMS value for vertical,

longitudinal and lateral acceleration respectively. Based on the polynomial fit for the

data points, a quadratic relation in observed for all three acceleration components. High

correlation of determination of $R^2 = 0.99$ for all three figures indicates 99% of the

variance in PCRMS is accounted for by the quadratic fit. For Figure 4-4, 4-5, and 4-6 the

error of fit was 4.58%, 4.467% and 6.37% respectively. These values suggest that a

quadratic fit is a reliable relation between PCRM and PCRMS for all three acceleration

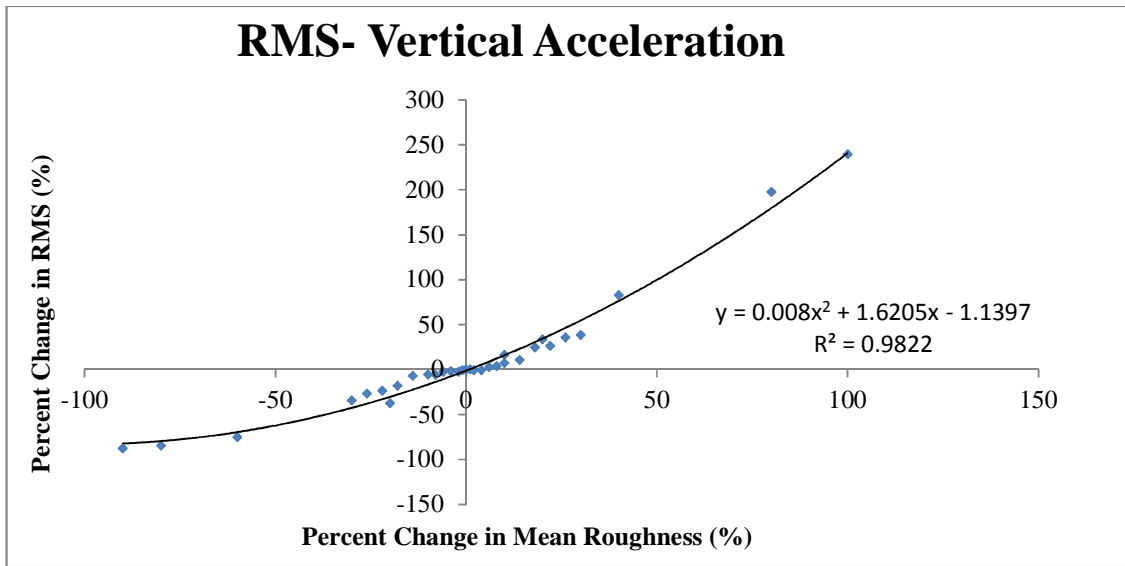components when variance is extended to ±100%.

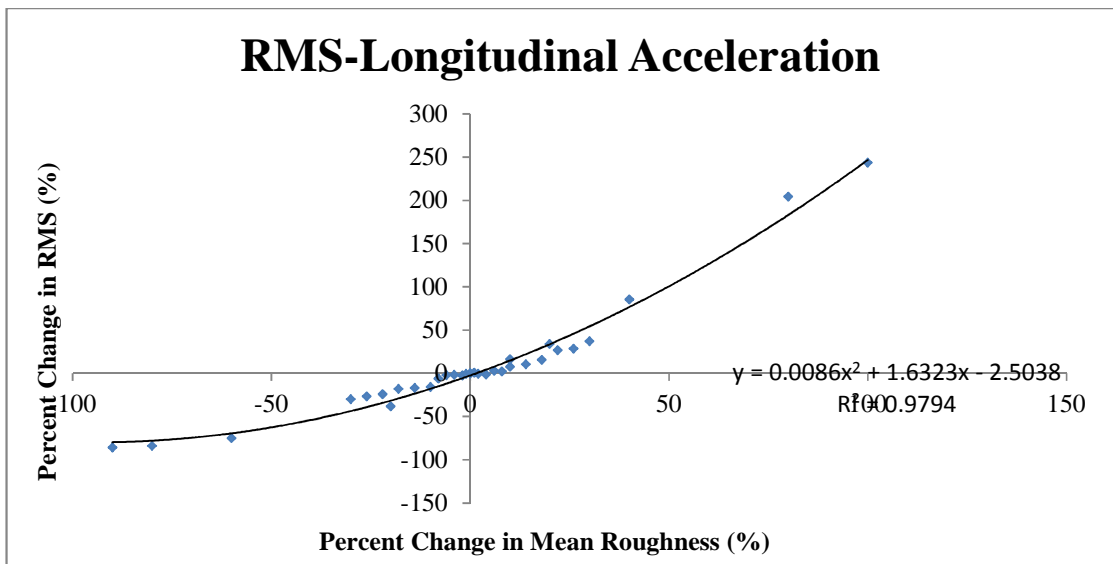Figure 4-4: Change in RMS of Vertical Acceleration vs. Large Variation of Mean Roughness

Figure 4-5: Percent Error in RMS of Longitudinal Acceleration with Large Variation Mean Roughness
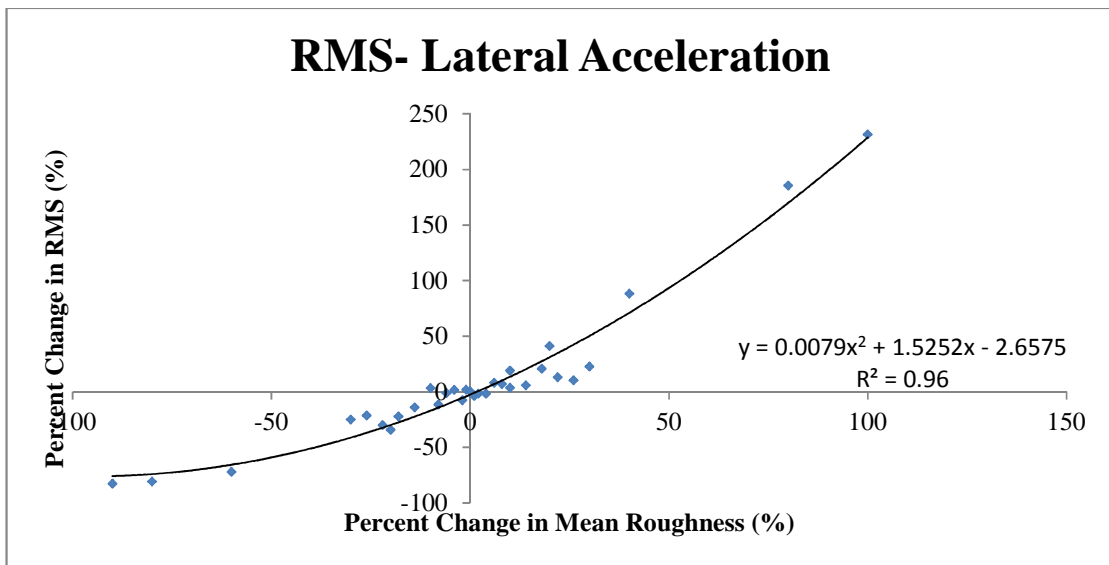
RMS- Lateral Acceleration

$y = 0.0079x^2 + 1.5252x - 2.6575$

$R^2 = 0.96$

Figure 4-6: Percent Error in RMS of Lateral Acceleration with Large Variation of Mean Roughness

4.4 Discussion

Results from the simulation show that there is a linear relation when small percentage change in mean roughness was plotted versus percent change in the RMS of the acceleration for variance up to ±30%. For the linear response, it was shown that for every 1.0% change in the mean roughness, the RMS value changes by about 0.65%. It is also noted that the R^2 value and error of the fit of the lateral acceleration were significantly higher than the vertical and longitudinal components. When the percent change in the mean was increased to ±100%, the observed effects departure from a linear relation. A quadratic relation was observed.

CHAPTER 5

SUMMARY AND CONCLUSION

The effect of varying roughness of road profiles on vehicle model was studied in this thesis. First, in an effort to extend the length of the experimentally acquired road profiles, a distribution function based methodology was developed to create road profile from the limited set of road data. The original road profile was first decomposed into three defining parameters, the roughness height, length and interval. Using best fit distribution functions that defined each of the three parameters, random numbers were generated to be used for road profile construction. A Mathematica program was used to assemble the random numbers into a spline curve which is then used in Virtial.Lab. An advanced vehicle model was updated with new hard-point data. Other updates include two differential models to accurately simulate the all-wheel-drive capability of the vehicle and a dynamic model of a trailer was also added. The trailer was added to match the conditions of the experimental tests and to improve the correlation of the results from the experimental tests and the simulation results.

The updated model was validated using the dynamic results obtained from the experimental tests conducted by the NATC. The results showed that the model is able to predict the RMS of vertical acceleration very well. The RMS results from the simulation fell between the two dynamic results and thus the updated model was validated. With the addition of the trailer model, increase in the accuracy of the models ability to predict the longitudinal acceleration was expected. Only slight increase in accuracy was observed and more refinement is necessary before more improvement can be expected.

The methodology of creating road profile was validated by using the updated model with both the original and the new road profile. The result shows that the model under predicts the RMS for vertical acceleration when using the new road profile compared to the original road profile. It was also shown that the uncertainty of simulation using the new road profile was much tighter than the dynamic results. If more road roughness data was available to fit the distributions, then the results would have been closer to the results obtained from the original road profile. Even with the limited road data, the methodology for creating road profile from distribution has shown to generate road profiles that produce results very similar to the original road profile and thus the methodology was validated.

Using the methodology of creating road profile, a parametric study was conducted to assess the sensitivity of road profile on vehicle models. The distribution function describing the roughness height was changed to a more convenient function so the road profiles could be generated easier. Road profiles were created with varying mean roughness value and used in the vehicle model. The results were compared to a control road profile that was created using the roughness value of the original road profile. The results from the simulation show that there is a linear relation when small percentage change in mean roughness was plotted versus percent change in the RMS of the acceleration for variance up to ±30%. For the linear response, it was shown that for every 1.0% change in mean roughness, 0.65% change in the RMS was observed. When the percent change in mean was increased to ±100% the observed effects departed from a linear relation and a quadratic relation was observed. With these results, some insights

have been gained on how the variability in the road profile affects the vehicle simulation results.

While the vertical acceleration data extracted from the updated model compare well with the dynamic data, further refinements to the model can be made to increase the accuracy of the results. These refinements include adding a breaking mechanism that exists between the HMMWV and the trailer. Translation is allowed at this location because of the breaking mechanism and might add valuable information to the model. Zeman (2009) suggested that if more detailed tire information is available then a better tire model that is suited for high frequency road inputs should be used. Since such information was not available, same tire model was used as Zeman (2009). Several improvements to the trailer model can also be made including getting real test data for the spring stiffness for the trailer suspension and getting more accurate center of gravity and moment of inertia values for the various components in the trailer.

If improvements to the vehicle model can be implemented, the model will be able to produce more accurate simulation results. It is hoped that with more improvements the vehicle model will allow to perform component level durability analysis in the trailer. With this ultimate goal in mind, further research to improve the model is currently being conducted.

REFERENCES

Aardema, J. 1988. Failure Analysis of the Lower Rear Ball Joint on the High-Mobility Multipurpose Wheeled Vehicle (HMMWV). United States Army Tank-Automotive Command Research, Development, and Engineering Center.

AM General. 2010. Corporate Video 2010. http://www.amgeneral.com/corporate/media/ (accessed November 2, 2010).

Bogsjo, K. 2006. Development of analysis tools and stochastic models of road profiles regarding their influence on heavy vehicle fatigue. *Vehicle System Dynamics*, 44:1,780-790.

Dodds, C.J., and Robson, J. D. (1973). The description of road surface roughness. *Journal of Sound and Vibration*: 31(2), 175-183.

Engineering Statistics Handbook, 2003. *Kolmogorov-Smirnov Goodness-of-Fit Test*. http://www.itl.nist.gov/div898/handbook/eda/section3/eda35g.htm (accessed 4/11/2011).

Figliola, R. S. and Beasley, D. E. 2006. *Theory and Design for Mechanical Measurements*. 4th ed. Hoboken, John Wiley & Sons, Inc.

Haug, E.J. 1989. *Computer-Aided Kinematics and Dynamics of Mechanical Systems*. Boston, MA; Allyn and Bacon.

Heath, A. N. 1989. Modelling and simulation of road surface roughness. *Vehicle Systems Dynamics*: 18,275-284.

HMMWV, Image retrieved from www.defense-update.com (accessed April 7, 2011).

Hussien, A. H., Shabana A. A., Tsung, W., Fetcho, M. R. 2000. Dynamic and Vibration Analysis of a Vehicle Rear Axle System. *Vehicle System Dynamics*. 33:4,205-231.

Kang, D., Park. K, Heo, S., Ryu, Y., and Jeong, J. 2009 *International Journal of Precision Engineering and Manufacturing*. 11:2, 265-272.

L'Ecuyer, P and Simard. R. 2007. A C Library for Emperical Testing of Random Number Generators. *ACM Transaction on Mathematical Software*. 33:4, Article 22.

LMS International. (2010). Virtual.Lab Rev 9-SL1 User Guide.

Michael W. S., Steve M. K. 1998. The Little Book of Profiling. The Regent of the University of Michigan.

MathWave Technologies. 2010. EasyFit Professional, Help files.

MIL-STD-810G. 2008. http://www.everyspec.com/ (accessed January 1, 2011).

Mousseau C.W., Laursen, T.A., Lidberg, M. and Tayloer, R.L. 1999. Vehicle Dynamics Simulations With Coupled Multibody and Finite Element Models. *Finite Elements in Analysis and Design*:31 295-315.

NATC. November 2, 2009. *Terrain Profiling*. http://www.natcht.com/Test_Course_Descriptions.htm (accessed November 2, 2010).

Perm, H. 1998. A Laser Based Highway-Speed Road Profile measuring system. *Vehicle System Dynamics.*: 17, 300-304.

Prescott, W. and Langhlin, J. 2007. Implementation and Usage of Design Sensitivity Analysis in Multibody Dynamics Software. *Multibody Dynamics 2007, ECCOMAS Thematic Conference.*

Rouillard, V., Sek, M. A., Bruscella, B. 2001. Simulation of Road Surface Profiles. *Journal of Transportation Engineering*. (May/June):247-253.

Schutt Industries, LTT Common 22 Shop Set Trailer. schuttindustries.com (accessed April 7, 2011).

Differential gear, *Line art diagram of a differential gear.* http://commons.wikimedia.org/wiki/File:Differential_gear_(PSF).png (accessed April 7, 2011).

Wolfram Research, Inc., Mathematica, Version 8.0, Champaign, IL (2010).

Zeman, Jonathan. 2009. A V-DMAC Case Study of High Mobility Multipurpose Wheeled Vehicle Driving on Rough Terrain, University of Iowa.

APPENDIX A. Mathematica Code for Rode Roughness Simulation

Mathematica Code

```
RoadRoughness=ReadList["H:\\Height.csv"];        "Input: Reads roughness height
input data"
LengthOfBump=ReadList["H:\\Length.csv"];         "Input: Reads roughness length
input data"
BumpInterval=["H:\\Interval.csv"];               "Input: Reads roughness interval input
data"
num= Length[RoadRoughness];                      "defines total number of data points"
total= num 4;
Clear[θ,a,b,c]
a=RoadRoughness;
b=LengthOfBump;
c=BumpInterval;
θ=0;
RoadProfile=Table[{0,0},{total}];
pt1=pt2=pt3=pt4=Table[{0,0},{num}];
Do[pt1[[i]]={θ,0};                               "Builds each section of the road profile"
 pt2[[i]]={ θ,a[[i]]};
 pt3[[i]]={ θ +b[[i]],a[[i]]};
 pt4[[i]]={ θ +b[[i]],0};
 θ = θ +b[[i]]+c[[i]];,{i,1,num}]


Clear[RoadProfile]
RoadProfile={{0,0}};
Do[                                              "Combines sections of the road profile"
 RoadProfile=Append[RoadProfile,pt1[[i]]];
 RoadProfile=Append[RoadProfile,pt2[[i]]];
 RoadProfile=Append[RoadProfile,pt3[[i]]];
 RoadProfile=Append[RoadProfile,pt4[[i]]];
 ,{i,1,num}]
{x,y}=Transpose[RoadProfile];

str=OpenWrite["H:\\Final Road\x.tmp"]            "Output: Writes x-axis of road profile to
file"
WriteString[str,x]
Close[str]

str=OpenWrite["H:\\Final Road\y.tmp"]            "Output: Writes y-axis of road profile to
file"
WriteString[str,y]
Close[str]
```